Charles University in Prague
Faculty of Mathematics and Physics

**DIPLOMA THESIS**

Vojtěch Pleskot

# Angular Correlations in the Higgs Boson Decays

Institute of Particle and Nuclear Physics
Supervisor: RNDr. Tomáš Davídek, PhD.
Study programme: Physics, Nuclear and Subnuclear Physics

I thank Tomáš Davídek very much for leading carefully my thesis and for his helpful attitude. I am also very grateful to him for having introduced me to software used in high energy physics. I would also like to thank Jiří Novotný for his precious advice and observations.

Prohlašuji, že jsem svou diplomovou práci napsal samostatně a výhradně s použitím citovaných pramenů. Souhlasím se zapůjčováním práce.

V Praze dne Vojtěch Pleskot

# Contents

Název práce: Úhlové korelace v rozpadech Higgsova bosonu
Autor: Vojtěch Pleskot
Katedra (ústav): Ústav Částicové a jaderné fyziky
Vedoucí diplomové práce: RNDr. Tomáš Davídek, PhD.
e-mail vedoucího: tomas.davidek@cern.ch
Abstrakt: Standardní model předpovídá, že Higgsův boson je jeden a má kombinovanou paritu CP = +1. V MSSM však existuje navíc i Higgsův boson, který má CP = −1. Práce se zabývá tím, jak určit CP Higgsova bosonu na základě úhlových korelací pionů a $\rho$-mesonů narozených v kaskádním rozpadu $H/A \to \tau^-\tau^+ \to \rho^-/\pi^-\nu_\tau\rho^+/\pi^+\bar{\nu}_\tau$. Výpočty jsou prováděné v prvním netriviálním řádu poruchové teorie. Dále se zkoumá možnost odlišení signálu (rozpad Higgsova bosonu) od nejvýznamnějšího pozadí (rozpad $Z$ bosonu). Zkoumané procesy jsou simulovány pomocí Monte Carlo generátorů Pythia a Tauola. Výstupy simulace jsou srovnány s vypočtenými teoretickými výsledky.
Klíčová slova: Higgsův boson, $\tau$-lepton, úhlové rozdělení, spin, parita

Title: Angular correlations in the Higgs boson decays
Author: Vojtěch Pleskot
Department: Institute of Particle and Nuclear Physics
Supervisor: RNDr. Tomáš Davídek, PhD.
Supervisor's e-mail address: tomas.davidek@cern.ch
Abstract: The Standard Model predicts existence of one Higgs boson with combined parity CP = +1. In MSSM there exist Higgs boson with CP = −1 in addition. The work develops one method of Higgs boson CP determination on the basis of angular correlations of pions and $\rho$-mesons born in cascade decay $H/A \to \tau^-\tau^+ \to \rho^-/\pi^-\nu_\tau\rho^+/\pi^+\bar{\nu}_\tau$. The calculations are done in the leading order of perturbation theory. Further, the possibility of signal (Higgs boson decay) and background ($Z$ boson decay) differentiation is studied. The processes in question are simulated using Monte Carlo generators Pythia and Tauola. Simulation outputs are compared with calculated theoretical results.
Keywords: Higgs boson, $\tau$-lepton, angular correlation, spin, parity

# Chapter 1

# Theoretical models

## 1.1 Higgs boson and $\tau$-lepton in SM and in MSSM

### 1.1.1 SM Higgs boson

Higgs boson is the last undiscovered particle predicted by the Standard Model (SM in what follows). It is used in the description of the so-called spontaneous electroweak symmetry breaking and in generation of particle masses through the famous Higgs mechanism. The point is that the exact SU(2) $\times$ U(1) electroweak symmetry predicts zero particle masses; this of course contradicts the experimental results - particles have masses - and thus the symmetry has to be broken. Higgs boson couplings relevant for the Higgs boson decays are proportional to particle masses[1]. Thus we can roughly say that it decays with the highest probability to pair of the heaviest particles over the threshold (given by Higgs boson mass $m_H$)[2]. For $m_H$ less than $\approx$ 120 GeV the Higgs boson decays dominantly to $b\bar{b}$ pair with BR $\approx$ 90%. The second decay $H \to \tau\tau$ have much lower but still non-negligible branching ratio (BR $\approx$ 10%) in this region. As $m_H$ increases the decay $H \to WW$ becomes more and more important and at $m_H \approx$ 120 GeV it starts to dominate. In the region 120GeV $< m_H <$ 160GeV at least one of the $W$ bosons is of course virtual. The $m_H$-dependence of branching ratios is in Figure 1.1 which was taken from [1]. For more information on the Electroweak theory see for example [2]. Direct measurement of Higgs boson existence (and of its mass) was made at the accelerator LEP at CERN and at the accelerator Tevatron in Fermilab. Four experiments at LEP concluded that Higgs boson with mass under 114.4 GeV does not exist with 95% confidence level ([3]). The results from Tevatron yield exclusion of the mass region $158 - 175$ GeV ([4]). The expectations of Higgs boson mass were made on the basis of perturbative high-order corrections. The theoretical results (including Higgs boson mass) were fitted to set of high-precision data. Thus the 95% one-sided confidence level upper limit on $m_H$ was set to 158 GeV. But sensitivity of these corrections to Higgs boson mass is weak (roughly speaking logarithmic)

[1] $g_{WWH} = gm_W$, $g_{ZZH} = gm_Z/2\cos\theta_W$, $g_{ffH} = -gm_f/2m_W$, where $f$ is arbitrary fermion

[2] It is exactly true for fermions; for gauge bosons the situation is a little more complicated - the decay to $W^+W^-$ dominates on all the region above it's threshold

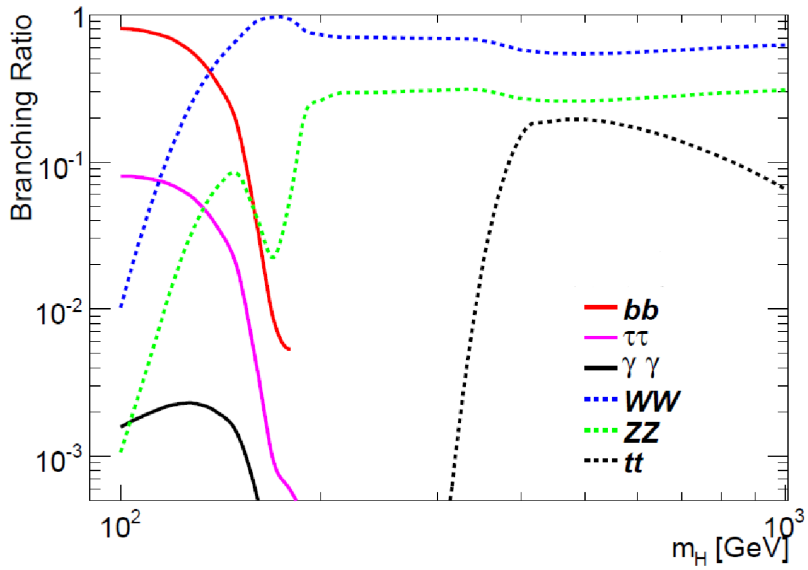


Figure 1.1: $m_H$ dependence of SM Higgs boson branching ratios

and thus their prediction power is not very strong. For more information see [4].

Only the exclusions of some Higgs boson masses were made so far. The question of it's existence or non-existence (and thus of it's mass of course) still remains open. It is the task of accelerator LHC at CERN to continue the Higgs boson searches. LHC provides protons collisions with center-of-mass energy 7 TeV at the moment but the nominal value is 14 TeV. By the end of the year 2012 enough data should be collected to either prove or exclude the Higgs boson existence up to the mass of 600 GeV.

### 1.1.2 Minimal Supersymmetric Standard Model

#### Introduction

The minimal supersymmetric extension of SM (i.e. Minimal Supersymmetric Standard Model, MSSM) states that each particle from the SM has it's supersymmetric partner (sparticle).[3] Supersymmetric particles have different spin (and therefore different statistical behavior) than their SM partners - SM bosons have MSSM fermionic partners and SM fermions have MSSM bosonic partners. There are two complex Higgs doublets in MSSM ($H_1$, $H_2$) and five physical Higgs bosons (three of eight original Higgs fields are eliminated as Goldstone bosons to generate three gauge boson masses): two of them are electrically charged ($H^+$, $H^-$) and three of them are neutral - CP-odd $A$, CP-even $H$ which is called heavy Higgs boson and another CP-even $h$, called light Higgs, which could be identified

[3] But the supersymmetry has to be broken so that the supersymmetric partners of SM particles had different masses; if the supersymmetry was not broken some MSSM particles would have been observed in the past which is obviously not the case

with SM Higgs boson. Supersymmetric fermionic partners of Higgs bosons are called Higgsinos. There is one vacuum expectation value associated with neutral component of each Higgs doublet ($v_1$, $v_2$). The original Higgs fields mix to form physical Higgs fields (mass eigenstates). There are two mixing angles. For example: $H^+ = \sin\beta(H_1^-)^* + \cos\beta H_2^+$, where $\tan\beta = v_2/v_1$. The other mixing angle $\alpha$ can be expressed in terms of the angle $\beta$ and CP-odd Higgs boson mass $m_A$. At the tree level the masses of MSSM Higgs bosons can be expressed in terms of these two free parameters ($m_A$, $\beta$) and of gauge bosons masses. Thus the Higgs bosons masses are given by:

$$m_{H^\pm}^2 = m_A^2 + m_W^2 \quad (1.1)$$

$$m_{H,h}^2 = \frac{1}{2}(m_A^2 + m_Z^2 \pm \sqrt{(m_A^2 + m_Z^2)^2 - 4m_A^2 m_Z^2 \cos^2 2\beta}) \quad (1.2)$$

On the basis of these formulae we can derive following constraints on the Higgs bosons masses:

$$m_{H^\pm} \geq m_W \quad (1.3)$$

$$m_H \geq m_A \geq m_h \quad (1.4)$$

$$m_h \leq m_Z \quad (1.5)$$

$$m_h^2 + m_H^2 = m_A^2 + m_Z^2 \quad (1.6)$$

From it follows that the light Higgs boson bare mass is smaller than that of $Z$ boson (which contradicts the experimental results because Higgs boson has not yet been observed). However, if radiative corrections are included, $m_h$ could increase to about 130 GeV.

One of new important concepts in MSSM is R-parity. It is internal symmetry whose value for each particle is defined to be

$$R = (-1)^{3B+L+2s} \quad (1.7)$$

where $B$, $L$ and $s$ are the particle's baryon number, lepton number and spin respectively. Thus $R = 1$ for all conventional matter particles and $R = -1$ for their superpartners. In MSSM the R-parity conservation is postulated. The postulate has these important consequences:

- In accelerator experiments, sparticles can only be produced in pairs
- The lightest sparticle (LSP) is stable and if it is electrically neutral it could be non-baryonic dark matter candidate
- The decay products of all other sparticles must contain an odd number of the lightest sparticles; and since the LSP have no electric or strong charge in MSSM they cannot be detected. In accelerator experiments at least $2m_{\mathrm{LSP}}$ missing energy has to be associated with each SUSY event.

For more information on the MSSM see [6], [7] and [8].

**MSSM Higgs bosons production processes in $pp$ collisions**

The Higgs bosons couplings to other particles are also functions of unknown mixing angle $\beta$ (in addition to other parameters). Thus the production (as well as decay) processes have to be discussed in the dependence of this parameter. In general there are four main MSSM Higgs production processes:

- gluon-gluon fusion: $gg \rightarrow h/H/A$
- vector boson fusion: $qq' \rightarrow q''q''' + W^*W^*/Z^*Z^* \rightarrow q''q''' + h/H$
- associated production with heavy quarks (i.e. $t$ or $b$ in final state): $gg/q\bar{q} \rightarrow q'\bar{q}' + h/H/A$
- associated production with vector boson: $q\bar{q}' \rightarrow W/Z + h/H$

The light Higgs boson is similar to that from SM and thus it's dominant production process is the gluon-gluon fusion. The CP-odd Higgs boson $A$ cannot be produced in the second and the fourth reaction because it does not couple to vector bosons in MSSM. As we said already the $H$ and $A$ Higgs bosons couplings depend on the parameter $\beta$. For low values of $\tan\beta$ (i.e. $\tan\beta \approx 3$ or less) $H$ and $A$ couplings to up-type quarks are enhanced and the dominant production process is gluon-gluon fusion, especially via the top quark loop. For high $\tan\beta$ (i.e. $\tan\beta \approx 30$ or greater) the couplings to down-type quarks are enhanced and the dominant production process is associated production with $b$-quarks, but gluon-gluon fusion via $b$-quark loop contributes significantly too.

**MSSM Higgs boson decays**

The light Higgs boson has couplings similar to SM Higgs boson whose decays were briefly discussed in Section 1.1.1. Here we are going to discuss the decays of $H$ and $A$ bosons. The heavy Higgs bosons decays strongly depend on $\tan\beta$. For low values of this parameter the couplings to up-type quarks are enhanced and (when allowed) the decay to pair of top quarks dominates. In lower mass region ($m_{H/A} \approx 130 - 300$ GeV) $A$ decays dominantly to $b\bar{b}$ and $\tau\tau$ (BR $\approx 90\%$ and BR $\approx 10\%$ respectively) and $H$ decays dominantly to $WW$, $b\bar{b}$, $ZZ$ and $hh$. For high values of $\tan\beta$ the couplings to down-type quarks are enhanced and the dominant decay processes are thus $H/A \rightarrow b\bar{b}$ with BR $\approx 90\%$ and $H/A \rightarrow \tau\tau$ with BR $\approx 10\%$ in practically all the allowed mass region.

### 1.1.3 $\tau$-lepton

$\tau$ is the heaviest lepton in SM. It was discovered in 1975 in the laboratory SLAC (USA) at the $e^+e^-$ accelerator SPEAR. It's neutrino was confirmed much later - at the beginning of new millennium - in experiment DONUT in the laboratory FNAL (USA). $\tau$-lepton's mass is $m_\tau \approx 1.777$ GeV and thus it can decay hadronicaly in contrast to other leptons[4]. Thanks to the lepton universality it has the same basic properties as muon and electron apart from the mass. But the decay rate of the process $h \to \tau\tau$ is much bigger than that of processes $h \to ee$, $h \to \mu\mu$ due to the above mentioned fact that Higgs boson couplings to fermions is proportional to fermion masses. Thus we can write:

$$\Gamma(h \to \mu\mu) = \frac{m_\mu^2}{m_\tau^2}\Gamma(h \to \tau\tau) \tag{1.8}$$

$$\Gamma(h \to ee) = \frac{m_e^2}{m_\tau^2}\Gamma(h \to \tau\tau) \tag{1.9}$$

$\tau$ leptonic decays have branching ratio approximately 35% (17.4% for $\tau \to \mu\nu_\mu\nu_\tau$ and 17.8% for $\tau \to e\nu_e\nu_\tau$ thanks to the lepton universality). $\tau$-lepton hadronic decays have BR $\approx$ 65% and are dominated by $\tau \to \rho\nu_\tau$ process with BR $\approx$ 25%. The second most important hadronic decay is $\tau \to \pi\nu_\tau$ (BR $\approx$ 11%). The remaining hadronic decays are of little importance in the context of this thesis. For more information see [5]. MSSM $\tau$-lepton has the same behavior as in SM and thus all the discussion above is valid for it as well.

[4]The lightest charged hadron is $\pi$-meson with $m_\pi \approx 140$ MeV; this fact kinetically forbids muon ($m_\mu \approx 105$ MeV) and electron ($m_e \approx 0.5$MeV) to decay hadronicaly

# Chapter 2

# Angular Correlations

## 2.1 Introduction

In this section we are going to develop one method of Higgs boson CP measurement. As discussed in Section 1.1.2 there are two CP-even and one CP-odd Higgs bosons in MSSM. The method to be developed can distinguish CP-even from CP-odd Higgs boson on the basis of angular correlations of hadronic decay products of $\tau$-leptons born in Higgs boson decay. The directions of these hadrons (either $\pi$-meson or $\rho$-meson) are correlated due to the correlation of spins of the two $\tau$-leptons and due to the parity violation in weak interactions (neutrinos/antineutrinos are born left/right-handed in the $\tau^-/\tau^+$ decays). An instructive insight to the problem can give us considerations based on angular momentum quantum mechanical treating. The most important point is that spin-angular part of the wave function of $\tau$-leptons born in CP-odd Higgs boson decay is antisymmetric with respect to the $\tau$-leptons exchange:

$$|\tau^+\tau^-\rangle \quad \sim \quad \frac{1}{\sqrt{8\pi}}\Big(|\tau^-_\uparrow\rangle|\tau^+_\downarrow\rangle - |\tau^-_\downarrow\rangle|\tau^+_\uparrow\rangle\Big) \tag{2.1}$$

whereas in the case of CP-even Higgs boson it is symmetric

$$|\tau^+\tau^-\rangle \quad \sim \quad \frac{1}{\sqrt{8\pi}}(|\tau^-_\uparrow\rangle|\tau^+_\downarrow\rangle + |\tau^-_\downarrow\rangle|\tau^+_\uparrow\rangle) \tag{2.2}$$

if we choose appropriate orientation of axes of the Higgs boson rest frame with respect to the direction of $\tau$-leptons (see Section 2.2.1). The notation is such that for example $|\tau^-_\uparrow\rangle$ denotes $\tau$-lepton with third component of its spin oriented in the direction of $z$-axis of the Higgs boson rest frame and the remaining symbols are analogic. The relative sign propagates into the form of the overall angular distribution. Detailed study of this quantum mechanical problem is in Appendix A. The angular distribution can not only be used in the Higgs boson CP determination but also in distinguishing of the $h/H/A \to \tau\tau$ event from its main background in the region of not very high Higgs boson masses which is the

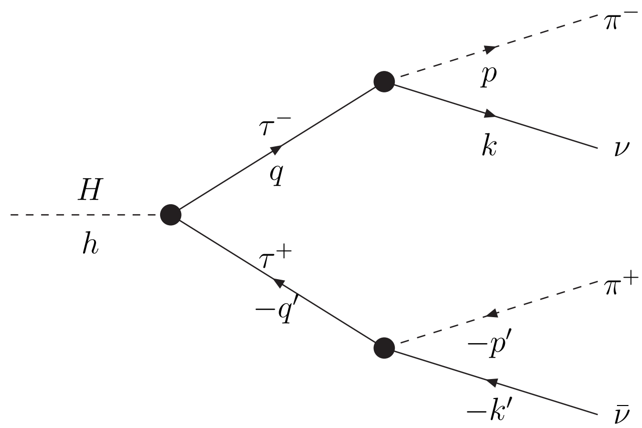


Figure 2.1: Feynman diagram of cascade Higgs boson decay into two pions and two neutrinos

process $Z \to \tau\tau$. Detailed study of all these angular distributions (on the basis of quantum field theory) are going to be performed in this thesis.

The difference between CP-odd and CP-even Higgs boson that is relevant for this thesis is that the CP-odd one has an additional Dirac $\gamma_5$ matrix in it's (Yukawa) coupling to $\tau$-leptons, namely:

$$\mathcal{L}_{\text{int}} = g_{A\tau\tau}\bar{\tau}\gamma_5\tau A \tag{2.3}$$

$$\mathcal{L}_{\text{int}} = g_{H\tau\tau}\bar{\tau}\tau H \tag{2.4}$$

For completeness, the notation that we are going to use in what follows is such that $H$ denotes CP-even Higgs boson (regardless of its type) and $A$ denotes the CP-odd one.

## 2.2 CP-even Higgs boson decays

### 2.2.1 Two pion final state

#### Squared matrix element

In this section we are going to calculate the angular distribution of products of process

$$H \to \tau^-\tau^+ \to \nu\pi^-\bar{\nu}\pi^+ \tag{2.5}$$

Tree level Feynman diagram of this process is in Fig. 2.1. In all the thesis we will neglect the higher-order perturbative corrections. We will express the result as a function of three independent angles whose meaning is as follows (see also Fig. 2.2):

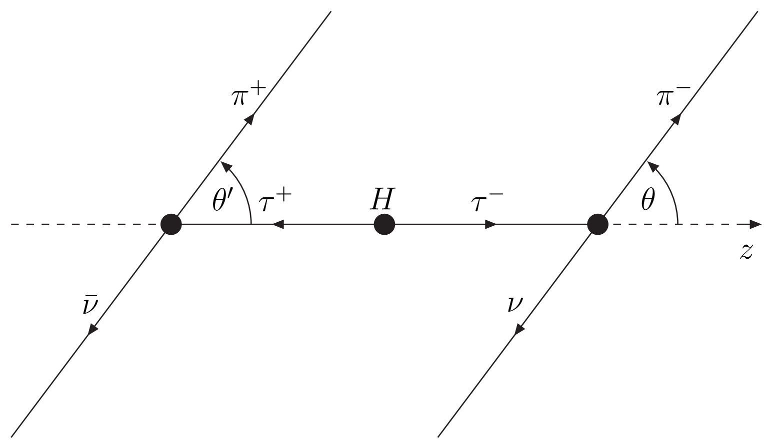


Figure 2.2: Geometry of the Higgs boson decay

- $\theta$ is polar angle of $\pi^-$ in $\tau^-$ rest frame (all the three axes of this frame has the same directions as those of Higgs boson rest frame)
- $\theta'$ is polar angle of $\pi^+$ in $\tau^+$ rest frame (all the three axes of this frame has the same directions as those of Higgs boson rest frame)
- $\phi$ is azimuthal angle between $\pi^-$ and $\pi^+$ transverse components directions (transverse with respect to the $z$-axis) in any frame ($\tau^-$, $\tau^+$ or $H$ rest frame) - thanks to the fact that movement of $\tau$-leptons is in the $z$-axis only, transverse components of pions momenta are not influenced by Lorentz boosts. We choose the frames such that the decay $\tau^- \rightarrow \pi^- \nu_\tau$ is in $x - z$ plane. Then the angle $\phi$ is azimuthal angle of $\pi^+$ in $\tau^+$ rest frame.

We will use the approximation of very narrow $\tau$-lepton decay width, in other words we will consider the $\tau$-leptons to be on-shell. We explain what we mean:

Relevant form of the fermion propagator in momentum representation is:

$$\mathrm{S_F}(q) \quad = \quad \frac{\not{q} + m_f}{q^2 - m_f^2 + i m_f \Gamma_f} \tag{2.6}$$

where $m_f$, $\Gamma_f$ are the fermion's mass and decay width respectively. Considering that the $\tau$-lepton decay width is very narrow we approximate the square of non-matrix part of the propagator by $\delta$-function, i.e. we do the substitution

$$\left| \frac{1}{q^2 - m_f^2 + i m_f \Gamma_f} \right|^2 \approx \frac{1}{P} \delta(q^2 - m_\tau^2) \tag{2.7}$$

where $P$ is a constant factor with dimension of square of mass. Since are aim is to calculate the angular distribution we do not care about value of this overal constant factor. Thus in the square of matrix element the nominators of $\tau$-lepton propagators will remain untouched whereas the product of two denominators yields $\delta$-function in this approximation. Thanks to this $\delta$-function we are allowed to replace $q^2$ by $m_\tau^2$ in all the squared matrix element. Since we use this equality ($q^2 = m_\tau^2$) we effectively assume the $\tau$-leptons to be on-shell although we describe them by propagator (which is in general related to off-shell particles).

Matrix element of $\tau$-lepton decay is:

$$\mathcal{M}(\tau^- \to \pi^- \nu_\tau) \quad = \quad -G_F \cos\theta_C f_\pi \bar{u}_L(k) \not{p}(1-\gamma_5)u(q) \tag{2.8}$$

where $G_F$ is Fermi weak constant, $\theta_C$ is Cabbibo angle and $f_\pi$ is pion decay constant. For details see [2]. Taking into account (2.8), matrix element of the whole process is:

$$\begin{aligned}\mathcal{M} &= g_{H\tau\tau}(-G_F \cos\theta_C f_\pi)^2 \times \bar{u}_L(k)\not{p}(1-\gamma_5)\frac{1}{\not{q}-m_\tau}\,\frac{1}{-\not{q}'-m_\tau}\not{p}'(1-\gamma_5)v_R(k') \\ &= g_{H\tau\tau}(-G_F \cos\theta_C f_\pi)^2 \times 4\bar{u}_L(k)\not{p}\frac{1}{\not{q}-m_\tau}\,\frac{1}{-\not{q}'-m_\tau}\not{p}'v_R(k')\end{aligned} \tag{2.9}$$

Let us define:

$$C \quad \equiv \quad \left(g_{H\tau\tau}(-G_F \cos\theta_C f_\pi)^2\right)^2 \frac{16}{R}\, \delta(q^2 - m_\tau^2)\delta(q'^2 - m_\tau^2) \tag{2.10}$$

where constant factor $R$ is remnant of the denominators of the propagators. Thus the squared matrix element can be written in the following way:

$$\begin{aligned}|\mathcal{M}|^2 = C \times \bar{v}_R(k')\not{p}'(-\not{q}'+m_\tau)(\not{q}+m_\tau)\not{p}u_L(k) \times \\ \times\bar{u}_L(k)\not{p}(\not{q}+m_\tau)(-\not{q}'+m_\tau)\not{p}'v_R(k')\end{aligned} \tag{2.11}$$

After detailed calculation given in Appendix B.1 we obtain the following result:

$$\begin{aligned}|\mathcal{M}|^2 \quad = \quad & C \times 2m_\tau^6\Big(2(q\cdot k)(q\cdot k') + 2(k'\cdot q')(k\cdot q') + \\ & +(2(q\cdot q') - 2m_\tau^2)(k\cdot k') - 2(q\cdot k')(k\cdot q') - 2(q\cdot k)(q'\cdot k')\Big)\end{aligned} \tag{2.12}$$

**Scalar products**

Due to the Lorentz-invariance of scalar product of two four-vectors we can evaluate different terms appearing in $|\mathcal{M}|^2$ in different reference frames (these frames will be the rest frames of $\tau$-leptons and of Higgs boson). We have to calculate these scalar products:

$$(k\cdot q), \quad (k'\cdot q'), \quad (k\cdot q'), \quad (q\cdot k'), \quad (q\cdot q'), \quad (k\cdot k') \tag{2.13}$$

In order to evaluate the products we will boost the vectors $q$ and $q'$ to the rest frames of $\tau^+$ and $\tau^-$ respectively and the vector $k'$ to the rest frame of $\tau^-$. We will use following notation:

- $\beta$ is the velocity of $\tau^-$ in CMS of the Higgs boson and $\gamma$ is the corresponding Lorentz $\gamma$-factor
- $\beta' = -\beta$ is the velocity of $\tau^+$ in CMS of the Higgs boson and $\gamma'$ is the corresponding Lorentz $\gamma$-factor
- subscript says in what frame the corresponding object is expressed (for example $k_{\mathrm{CMS}\tau^+}$ means the four-vector of neutrino expressed in $\tau^+$ rest frame).

Detailed calculation of the scalar products (2.13) is given in Appendix B.2. Here we present the results:

$$\begin{aligned}
(k \cdot q) &= \left|\vec{k}_{\mathrm{CMS}\tau^-}\right| m_\tau && (2.14a)\\
(k' \cdot q') &= \left|\vec{k'}_{\mathrm{CMS}\tau^+}\right| m_\tau && (2.14b)\\
(k \cdot q') &= \left|\vec{k}_{\mathrm{CMS}\tau^-}\right| \gamma \frac{m_H}{2}\left(1 - 2\beta\cos\theta + \beta^2\right) && (2.14c)\\
(k' \cdot q) &= \left|\vec{k'}_{\mathrm{CMS}\tau^+}\right| \gamma \frac{m_H}{2}\left(1 + 2\beta\cos\theta' + \beta^2\right) && (2.14d)\\
(q \cdot q') &= \frac{m_H^2 - 2m_\tau^2}{2} && (2.14e)\\
(k \cdot k') &= \left|\vec{k}_{\mathrm{CMS}\tau^-}\right| \left|\vec{k'}_{\mathrm{CMS}\tau^+}\right| \times \left(\frac{1+\beta^2}{1-\beta^2}(1 - \cos\theta\cos\theta') + \right.\\
&\left. + \frac{2\beta}{1-\beta^2}\left(\cos\theta' - \cos\theta\right) - \sin\theta\sin\theta'\cos\phi\right) && (2.14f)
\end{aligned}$$

where $\left|\vec{k}_{\mathrm{CMS}\tau^-}\right|$ and $\left|\vec{k'}_{\mathrm{CMS}\tau^+}\right|$ can be expressed in terms of particle masses, see (B.17a).

#### Integration of the squared matrix element

We instituted the previously calculated scalar products in (2.12) using the software Mathematica. The result is:

$$|\mathcal{M}|^2 = C \times \frac{1}{2} m_\tau^4 (m_H^2 - 4m_\tau^2)(m_\tau^2 - m_\pi^2)^2 (1 + \cos\theta\cos\theta' - \sin\theta\sin\theta'\cos\phi) \quad (2.15)$$

Now, we have to integrate it over the Lorentz invariant phase space of four particles ($\mathrm{LIPS}_4$). Details of the integration are in Appendix B.3. The result is:

$$\mathrm{d}\Gamma = \frac{1}{2m_H}\frac{1}{\pi^2(8\pi)^4}\sqrt{1 - \frac{4m_\tau^2}{m_H^2}}\frac{\left|\vec{p}_{\mathrm{CMS}\tau^-}\right|\left|\vec{p'}_{\mathrm{CMS}\tau^+}\right|}{m_\tau^2}|\mathcal{M}|^2 \mathrm{d}q^2\mathrm{d}q'^2\mathrm{d}\cos\theta\mathrm{d}\cos\theta'\mathrm{d}\phi \quad (2.16)$$

#### Final result

The desired angular distribution of two pions born in decay (2.5) is thus:

$$\frac{1}{\Gamma}\frac{\mathrm{d}\Gamma}{\mathrm{d}\cos\theta\mathrm{d}\cos\theta'\mathrm{d}\phi} = \frac{1}{8\pi}(1 + \cos\theta\cos\theta' - \sin\theta\sin\theta'\cos\phi) \quad (2.17)$$

### 2.2.2 One pion and one $\rho$-meson final state

In this section we are going to present the result of calculation of angular distribution of one pion and one $\rho$-meson born in the cascade decay

$$H \to \tau^-\tau^+ \to \nu\rho^-\bar{\nu}\pi^+ \tag{2.18}$$

Our notation will be the same (i.e. the angle variables now relate to $\rho^-$-meson instead of to $\pi^-$-meson). We will not give details of the calculation because it is similar to the case of two pion final state (see Section 2.2.1). There is just one difference between the two cases - $\rho$-meson is vector meson (whereas pion is pseudoscalar) and thus the $\tau$-lepton decay matrix element has the following form:

$$\mathcal{M}(\tau^- \to \rho^-\nu_\tau) \;=\; -G_F\cos\theta_C f_\rho \bar{u}_L(k)\not{\epsilon}^*(p,\lambda)(1-\gamma_5)u(q) \tag{2.19}$$

We can see that the $\rho$-meson polarization vector substituted the momentum in the matrix element (compare with (2.8)).

Matrix element of the whole process is:

$$\begin{aligned}\mathcal{M} \;=\;& g_{H\tau\tau}(-G_F\cos\theta_C f_\pi)(-G_F\cos\theta_C f_\rho)\times\\ &\times\bar{u}_L(k)\not{\epsilon}^*(p,\lambda)(1-\gamma_5)\frac{1}{\not{q}-m_\tau}\,\frac{1}{-\not{q}'-m_\tau}\not{p}'(1-\gamma_5)v_R(k')\end{aligned} \tag{2.20}$$

Due to the presence of polarization vector in (2.20) there appears an additional term in the squared matrix element with respect to (2.11). We have to sum over three polarization states of the $\rho$-meson which gives:

$$\sum_{\lambda=1}^{3}\epsilon_\mu(p,\lambda)\epsilon^*_\nu(p,\lambda) \;=\; -g_{\mu\nu}+\frac{1}{m_\rho^2}p_\mu p_\nu$$

The term with $p_\mu p_\nu$ has exactly the same structure as (2.11) but the term with $g_{\mu\nu}$ is new with respect to (2.11). Nevertheless, we will not give details of the calculation of this term here.

After all the calculation machinery (including the narrow $\tau$ width simplification discussed in Section 2.2.1) the result is:

$$\begin{aligned}|\mathcal{M}|^2 \;=\;& C'\times\frac{1}{2m_\rho^2}m_\tau^2(m_\tau^2-m_\pi^2)(m_\tau^2-m_\rho^2)(m_H^2-4m_\tau^2)(m_\tau^2+2m_\rho^2)\times\\ &\times\left(1+\left(\frac{m_\tau^2-2m_\rho^2}{m_\tau^2+2m_\rho^2}\right)(\cos\theta\cos\theta'-\sin\theta\sin\theta'\cos\phi)\right)\end{aligned} \tag{2.21}$$

where

$$C' \;\equiv\; (g_{H\tau\tau}(-G_F\cos\theta_C f_\pi)(-G_F\cos\theta_C f_\rho))^2\,\frac{16}{R}\,\delta(q^2-m_\tau^2)\delta(q'^2-m_\tau^2) \tag{2.22}$$

The angular distribution of pion and $\rho$-meson from the process (2.18) is:

$$\frac{1}{\Gamma}\frac{\mathrm{d}\Gamma}{\mathrm{d}\cos\theta \mathrm{d}\cos\theta' \mathrm{d}\phi} = \frac{1}{8\pi}\left(1+\left(\frac{m_\tau^2-2m_\rho^2}{m_\tau^2+2m_\rho^2}\right)(\cos\theta\cos\theta'-\sin\theta\sin\theta'\cos\phi)\right) \quad (2.23)$$

We can see that the angular-dependent part is suppressed by a factor $(m_\tau^2-2m_\rho^2)/(m_\tau^2+2m_\rho^2)$ with respect to the two pion final state topology.

### 2.2.3 Two $\rho$-meson final state

We are going to present the result of calculation of angular distribution of two $\rho$-mesons born in the cascade decay

$$H \to \tau^-\tau^+ \to \nu\rho^-\bar{\nu}\rho^+ \quad (2.24)$$

Matrix element of this process is:

$$\begin{aligned}\mathcal{M} &= g_{H\tau\tau}(-G_F\cos\theta_C f_\rho)^2 \times \\ &\times \bar{u}_L(k)\not{\epsilon}^*(p,\lambda)(1-\gamma_5)\frac{1}{\not{q}-m_\tau}\,\frac{1}{-\not{q}'-m_\tau}\not{\epsilon}^*(p',\lambda')(1-\gamma_5)v_R(k')\end{aligned} \quad (2.25)$$

Now, both pion momenta are substituted by $\rho$-meson polarization vectors in the matrix element. This yields two polarization sums and three different terms in the squared matrix element (two of them has the same structure as in one pion and one $\rho$-meson case). We will not give details of the calculation of the third term. We just present the result:

$$\begin{aligned}|\mathcal{M}|^2 &= C'' \times \frac{1}{2m_\rho^4}(m_H^2-4m_\tau^2)(m_\tau^2-m_\rho^2)^2(m_\tau^2+2m_\rho^2)^2 \times \\ &\times \left(1+\left(\frac{m_\tau^2-2m_\rho^2}{m_\tau^2+2m_\rho^2}\right)^2(\cos\theta\cos\theta'-\sin\theta\sin\theta'\cos\phi)\right)\end{aligned} \quad (2.26)$$

where

$$C'' \equiv \left(g_{H\tau\tau}(-G_F\cos\theta_C f_\rho)^2\right)^2\frac{16}{R}\,\delta(q^2-m_\tau^2)\delta(q'^2-m_\tau^2) \quad (2.27)$$

The angular distribution of two $\rho$-mesons born in the process (2.24) is:

$$\frac{1}{\Gamma}\frac{\mathrm{d}\Gamma}{\mathrm{d}\cos\theta \mathrm{d}\cos\theta' \mathrm{d}\phi} = \frac{1}{8\pi}\left(1+\left(\frac{m_\tau^2-2m_\rho^2}{m_\tau^2+2m_\rho^2}\right)^2(\cos\theta\cos\theta'-\sin\theta\sin\theta'\cos\phi)\right) \quad (2.28)$$

We can see that the angular-dependent part is suppressed by a factor $(m_\tau^2-2m_\rho^2)^2/(m_\tau^2+2m_\rho^2)^2$ with respect to the two pion final state topology.

## 2.3 CP-odd Higgs boson decays

As stated in Section 2.1 (equations (2.3),(2.4)), the CP-odd Higgs boson coupling to $\tau$-leptons differs from that of CP-even Higgs boson by an additional $\gamma_5$ apart from the magnitude of the coupling constant. Matrix element of it's decay to a pair of $\tau$-leptons reads:

$$\mathcal{M}(A \to \tau^-\tau^+) \;=\; g_{A\tau\tau}\bar{u}(q)\gamma_5 v(q') \tag{2.29}$$

In all this section we will use the same notation as in previous Section 2.2. In fact all the calculations are practically the same as before - there is just one difference: the additional $\gamma_5$ in the vertex (2.3) effectively changes the sign in front of $\tau^+$ momentum. Thus we may just slightly modify the previously obtained results in order to get the angular distribution of CP-odd Higgs boson decay. For example the matrix element of CP-odd Higgs boson decay with two pions in final state is:

$$\begin{aligned}\mathcal{M} \;=\; & g_{A\tau\tau}(-G_F\cos\theta_C f_\pi)^2 \times \\ & \times \bar{u}_L(k)\not{p}(1-\gamma_5)\frac{1}{\not{q}-m_\tau}\gamma_5\frac{1}{-\not{q}'-m_\tau}\not{p}'(1-\gamma_5)v_R(k')\end{aligned} \tag{2.30}$$

and the squared matrix element is:

$$\begin{aligned}|\mathcal{M}|^2 = & -\left(g_{A\tau\tau}(-G_F\cos\theta_C f_\pi)^2\right)^2\frac{16}{R}\,\delta(q^2-m_\tau^2)\delta(q'^2-m_\tau^2)\times \\ & \times\mathrm{Tr}\left(\not{k}'\frac{1+\gamma_5}{2}\not{p}'(-\not{q}'+m_\tau)\gamma_5(\not{q}+m_\tau)\not{p}\not{k}\frac{1+\gamma_5}{2}\not{p}(\not{q}+m_\tau)\gamma_5(-\not{q}'+m_\tau)\not{p}'\right) \\ = & D\times\mathrm{Tr}(\not{k}'\frac{1+\gamma_5}{2}\not{p}'(\not{q}'+m_\tau)(\not{q}+m_\tau)\not{p}\not{k}\frac{1+\gamma_5}{2}\not{p}(\not{q}+m_\tau)(\not{q}'+m_\tau)\not{p}')\end{aligned} \tag{2.31}$$

where

$$D \;\equiv\; \left(g_{A\tau\tau}(-G_F\cos\theta_C f_\pi)^2\right)^2\frac{16}{R}\;\delta(q^2-m_\tau^2)\delta(q'^2-m_\tau^2) \tag{2.32}$$

The expression (2.31) is really the same as (2.11) apart from the sign in front of the $\tau^+$ momentum $q'$ (and the overall constant factor of course).

### 2.3.1 Two pion final state

The process in question is:

$$A \to \tau^-\tau^+ \to \nu\pi^-\bar{\nu}_\tau\pi^+ \tag{2.33}$$

Matrix element of this process is in equation (2.30). The result is:

$$|\mathcal{M}|^2 \;=\; D\times\frac{1}{2}m_\tau^4 m_H^2(m_\tau^2-m_\pi^2)^2(1+\cos\theta'\cos\theta+\sin\theta\sin\theta'\cos\phi) \tag{2.34}$$

The angular distribution of two pions born in the decay (2.33) is:

$$\frac{1}{\Gamma}\frac{\mathrm{d}\Gamma}{\mathrm{d}\cos\theta\mathrm{d}\cos\theta'\mathrm{d}\phi} \;=\; \frac{1}{8\pi}\left(1+\cos\theta\cos\theta'+\sin\theta\sin\theta'\cos\phi\right) \tag{2.35}$$

### 2.3.2 One pion and one $\rho$-meson final state

The process in question is:

$$A \to \tau^-\tau^+ \to \nu\rho^-\bar{\nu}_\tau\pi^+ \tag{2.36}$$

Matrix element of this process is:

$$\begin{aligned}\mathcal{M} &= g_{A\tau\tau}(-G_F\cos\theta_C f_\pi)(-G_F\cos\theta_C f_\rho)\times \\ &\times\bar{u}_L(k)\not{\epsilon}^*(p,\lambda)(1-\gamma_5)\frac{1}{\not{q}-m_\tau}\gamma_5\frac{1}{-\not{q}'-m_\tau}\not{p}'(1-\gamma_5)v_R(k')\end{aligned} \tag{2.37}$$

The result is:

$$\begin{aligned}|\mathcal{M}|^2 &= D'\times\frac{1}{2m_\rho^2}m_H^2m_\tau^2(m_\tau^2-m_\pi^2)(m_\tau^2-m_\rho^2)(m_\tau^2+2m_\rho^2)\times \\ &\times\left(1+\left(\frac{m_\tau^2-2m_\rho^2}{m_\tau^2+2m_\rho^2}\right)(\cos\theta\cos\theta'+\sin\theta\sin\theta'\cos\phi)\right)\end{aligned} \tag{2.38}$$

where

$$D' \equiv (g_{A\tau\tau}(-G_F\cos\theta_C f_\pi)(-G_F\cos\theta_C f_\rho))^2\,\frac{16}{R}\,\delta(q^2-m_\tau^2)\delta(q'^2-m_\tau^2) \tag{2.39}$$

The angular distribution of pion and $\rho$-meson born in the decay (2.36) is:

$$\frac{1}{\Gamma}\frac{\mathrm{d}\Gamma}{\mathrm{d}\cos\theta\mathrm{d}\cos\theta'\mathrm{d}\phi} = \frac{1}{8\pi}\left(1+\left(\frac{m_\tau^2-2m_\rho^2}{m_\tau^2+2m_\rho^2}\right)(\cos\theta\cos\theta'+\sin\theta\sin\theta'\cos\phi)\right) \tag{2.40}$$

### 2.3.3 Two $\rho$-mesons final state

The process in question is:

$$A \to \tau^-\tau^+ \to \nu\rho^-\bar{\nu}_\tau\rho^+ \tag{2.41}$$

Matrix element of this process is:

$$\begin{aligned}\mathcal{M} &= g_{A\tau\tau}(-G_F\cos\theta_C f_\rho)^2\times \\ &\times\bar{u}_L(k)\not{\epsilon}^*(p,\lambda)(1-\gamma_5)\frac{1}{\not{q}-m_\tau}\gamma_5\frac{1}{-\not{q}'-m_\tau}\not{\epsilon}^*(p',\lambda')(1-\gamma_5)v_R(k')\end{aligned} \tag{2.42}$$

The result is:

$$\begin{aligned}|\mathcal{M}|^2 &= D''\times\frac{1}{2m_\rho^4}m_H^2(m_\tau^2-m_\rho^2)^2(m_\tau^2+2m_\rho^2)^2\times \\ &\times\left(1+\left(\frac{m_\tau^2-2m_\rho^2}{m_\tau^2+2m_\rho^2}\right)^2(\cos\theta'\cos\theta+\sin\theta\sin\theta'\cos\phi)\right)\end{aligned} \tag{2.43}$$

where

$$D'' \equiv \left(g_{A\tau\tau}(-G_F \cos\theta_C f_\rho)^2\right)^2 \frac{16}{R}\,\delta(q^2 - m_\tau^2)\delta(q'^2 - m_\tau^2) \tag{2.44}$$

The angular distribution of pion and $\rho$-meson born in the decay (2.36) is:

$$\frac{1}{\Gamma}\frac{\mathrm{d}\Gamma}{\mathrm{d}\cos\theta\mathrm{d}\cos\theta'\mathrm{d}\phi} = \frac{1}{8\pi}\left(1 + \left(\frac{m_\tau^2 - 2m_\rho^2}{m_\tau^2 + 2m_\rho^2}\right)^2 (\cos\theta\cos\theta' + \sin\theta\sin\theta'\cos\phi)\right) \tag{2.45}$$

## 2.4 Summary of the results

Let us write and discuss the results obtained in this Chapter. General form of our angular distributions is

$$\frac{1}{\Gamma}\frac{\mathrm{d}\Gamma}{\mathrm{d}\cos\theta\mathrm{d}\cos\theta'\mathrm{d}\phi} = \frac{1}{8\pi}\left(1 + F \times (\cos\theta\cos\theta' + S \times \sin\theta\sin\theta'\cos\phi)\right) \tag{2.46}$$

where the factors $F$ and $S$ are summarized in Table 2.1. From this table we can see that

| | CP-even Higgs boson | | CP-odd Higgs boson | |
|---|---|---|---|---|
| hadrons | F | S | F | S |
| $\pi^-\pi^+$ | 1 | -1 | 1 | 1 |
| $\rho^-\pi^+$ | $\left(\frac{m_\tau^2-2m_\rho^2}{m_\tau^2+2m_\rho^2}\right)$ | -1 | $\left(\frac{m_\tau^2-2m_\rho^2}{m_\tau^2+2m_\rho^2}\right)$ | 1 |
| $\rho^-\rho^+$ | $\left(\frac{m_\tau^2-2m_\rho^2}{m_\tau^2+2m_\rho^2}\right)^2$ | -1 | $\left(\frac{m_\tau^2-2m_\rho^2}{m_\tau^2+2m_\rho^2}\right)^2$ | 1 |

Table 2.1: Parameters of angular distributions

the presence of $\rho$-mesons in final state results in suppression of the angular-dependence of the distribution with respect to the two pion final state topology. And we can also see (which is our main goal) that CP-odd and CP-even Higgs boson differ in the sign in front of the term $\sin\theta\sin\theta'\cos\phi$. We can see that CP-even Higgs boson prefers opposite directions of transverse momenta components of final state hadrons whereas the CP-odd one prefers the final state hadrons to have the same directions of these components. This fact in principle allows to distinguish Higgs bosons with combined parities CP = 1 and CP = $-1$. In reality this may not be possible because in hadrons collisions, which is the case of LHC, it is impossible to precisely reconstruct the Higgs boson rest frame due to the presence of two undetectable neutrinos in final state. We can use the so-called collinear approximation but in this approach we expect the transverse correlation to be destroyed.

## 2.5 $Z$ boson decay

As stated already the $Z$ boson decay to $\tau$-leptons represents the main background to Higgs boson decays to these leptons in the region of not very high Higgs boson masses. Our goal is to show that we can distinguish the background processes $Z \to \tau\tau$ from the signal ones on the basis of angular distribution of final-state hadrons. Contrary to the previous two cases we will consider only the two-pion-final-state decay here. We will see that the differentiation is possible thanks to the longitudinal spin effects and that the transverse spin effects are suppressed a lot even in the case of two pions in final state. If we do not consider the transverse spin effects (i.e. if we integrate the angular distribution over the angle $\phi$) the angular distributions appropriate to CP-even and CP-odd Higgs boson become the same. Thus the following discussion is valid for both CP-even and CP-odd Higgs boson.

The calculation of angular distribution in the case of $Z$ boson decay is more complicated because of the complicated $Z\tau\tau$ vertex and the vector-boson character of $Z$. Feynman diagram of this process is in Figure 2.3. We assigned $h$ as the momentum of decaying $Z$ boson and $\epsilon(h,\lambda)$ it's polarization vector where $\lambda = +, -, 0$ denotes respectively positive, negative and zero helicity. Matrix element of the process is given by:

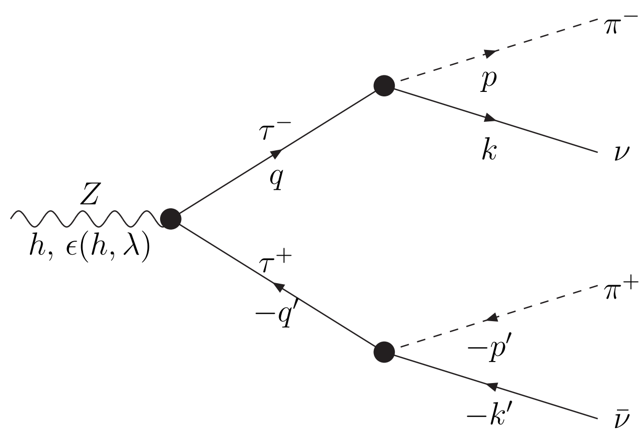


Figure 2.3: Feynman diagram of the cascade $Z$ boson decay into two pions and two neutrinos.

$$\begin{aligned}\mathcal{M} &= \frac{g}{2\cos\theta_W}(-G_F\cos\theta_C f_\pi)^2 \times \\ &\times \bar{u}_L(k)\not{p}(1-\gamma_5)\frac{1}{\not{q}-m_\tau}\not{\epsilon}(h,\lambda)(v-a\gamma_5)\frac{1}{-\not{q}'-m_\tau}\not{p}'(1-\gamma_5)v_R(k') \qquad (2.47)\end{aligned}$$

where

$$v = -\frac{1}{2} + 2\sin^2\theta_W \approx -0.19$$

$$
\begin{aligned}
a &= -\frac{1}{2} \\
\theta_W &\approx 23^\circ
\end{aligned}
\tag{2.48}
$$

We will not perform the calculation of the squared matrix element because it is somewhat lengthy and all the techniques are the same as before. Contrary to Higgs bosons cases there appear terms like $\mathrm{Tr}(\not{k}'\not{\epsilon}^*\not{k}\not{\epsilon}\gamma_5)$ and $\mathrm{Tr}(\not{k}'\not{q}'\not{\epsilon}^*\not{q}\not{k}\not{\epsilon})$ in the squared matrix element. The expression of these traces in terms of our variables (angles $\theta$, $\theta'$ and $\phi$ defined as before) is tedious but it is feasible. After having expressed the individual terms we used Mathematica to simplify all the expression.

We calculated the decay of polarized $Z$ boson for each helicity state separately. The polarization vectors for individual helicity states expressed in $Z$ boson rest frame are:

$$\epsilon^\mu(h,+) = \frac{1}{\sqrt{2}}(0,1,i,0) \tag{2.49}$$

$$\epsilon^\mu(h,-) = \frac{1}{\sqrt{2}}(0,1,-i,0) \tag{2.50}$$

$$\epsilon^\mu(h,0) = (0,0,0,1) \tag{2.51}$$

The results are:

$$|\mathcal{M}(0)|^2 \sim 2v^2 m_\tau^6 (m_\tau^2 - m_\pi^2)^2 (1 + \cos\theta\cos\theta' - \sin\theta\sin\theta'\cos\phi) \tag{2.52}$$

$$
\begin{aligned}
|\mathcal{M}(+)|^2 &\sim \frac{1}{2} m_\tau^4 (m_\tau^2 - m_\pi^2)^2 (v^2 m_Z^2 - 2avm_Z^2\sqrt{1-\frac{4m_\tau^2}{m_Z^2}} + a^2(m_Z^2 - 4m_\tau^2)) \times \\
&\quad \times (1 - \cos\theta\cos\theta' - (\cos\theta' - \cos\theta))
\end{aligned}
\tag{2.53}
$$

$$
\begin{aligned}
|\mathcal{M}(-)|^2 &\sim \frac{1}{2} m_\tau^4 (m_\tau^2 - m_\pi^2)^2 (v^2 m_Z^2 + 2avm_Z^2\sqrt{1-\frac{4m_\tau^2}{m_Z^2}} + a^2(m_Z^2 - 4m_\tau^2)) \times \\
&\quad \times (1 - \cos\theta\cos\theta' + (\cos\theta' - \cos\theta))
\end{aligned}
\tag{2.54}
$$

From these expressions we can see that square of the matrix element $\mathcal{M}(0)$ (which is the only one that contains transverse spin correlation) is suppressed by factor $m_\tau^2/m_Z^2$ with respect to the others. In the case of unpolarized $Z$ boson decay we thus have:

$$
\begin{aligned}
\overline{|\mathcal{M}|^2} &\sim \frac{1}{3}(|\mathcal{M}(0)|^2 + |\mathcal{M}(+)|^2 + |\mathcal{M}(-)|^2) \\
&\sim \frac{1}{3} m_\tau^4 \left(m_\tau^2 - m_\pi^2\right)^2 \left(m_Z^2\left(a^2+v^2\right) - m_\tau^2\left(4a^2 - 2v^2\right)\right) \times \\
&\quad \times \left(1 + \frac{2avm_Z^2\sqrt{1-\frac{4m_\tau^2}{m_Z^2}}(\cos\theta' - \cos\theta)}{(m_Z^2(a^2+v^2) - m_\tau^2(4a^2-2v^2))} - \right. \\
&\quad - \frac{(m_Z^2(a^2+v^2) - m_\tau^2(4a^2+2v^2))}{(m_Z^2(a^2+v^2) - m_\tau^2(4a^2-2v^2))}\cos\theta\cos\theta' - \\
&\quad \left. - \frac{2v^2 m_\tau^2}{(m_Z^2(a^2+v^2) - m_\tau^2(4a^2-2v^2))}\sin\theta\sin\theta'\cos\phi\right)
\end{aligned}
\tag{2.55}
$$

It can be simplified if we neglect the terms proportional to $m_\tau^2/m_Z^2$:

$$\begin{aligned}\overline{|\mathcal{M}|^2} \sim\ & \frac{1}{3}m_\tau^4\left(m_\tau^2 - m_\pi^2\right)^2 m_Z^2\left(a^2+v^2\right)\times \\ & \times\left(1+\frac{2av}{a^2+v^2}(\cos\theta'-\cos\theta)-\cos\theta\cos\theta'\right)\end{aligned} \tag{2.56}$$

From this relation we can see that there are two things that make the difference between this angular distribution and that from the Higgs boson decay. First of all it is the sign in front of the product of the two cosines. It can be seen on Figures 3.7 and 3.8 that are 2-D histograms of the two cosines. Secondly there are the terms linear in cosines that were not present in the case of Higgs boson decays. It can also be seen on Figure 3.8 - one of the two "peaks" is higher than the other. It is thanks to the presence of these two terms and to the fact that the relative sign between them is negative.

This behavior of the angular distribution from $Z$-boson decay makes it possible to distinguish this background process from the signal one. We can conclude it even in situation when we do not know the exact polarization of $Z$-boson if we assume that the longitudinal polarization does not dominate very much over the other two polarizations. In this situation we can write:

$$\frac{1}{\Gamma}\frac{\mathrm{d}\Gamma}{\mathrm{d}\cos\theta\mathrm{d}\cos\theta'} = \frac{1}{4}(1-\cos\theta\cos\theta'+k(\cos\theta'-\cos\theta)) \tag{2.57}$$

where $k$ is constant factor that depends on the $Z$ boson polarization state.

# Chapter 3

# Simulation

## 3.1 General aspects of Monte Carlo methods

The Monte Carlo methods form a very large class of probabilistic computational algorithms based on repeated processing of randomly chosen inputs. Their use is advantageous if deterministic ("exact") result cannot be obtained because of the difficulty of it's computation. Thanks to the idea of Stanislaw Ulam the first serious use of a Monte Carlo method was made at Los Alamos Scientific Laboratory in forties during the work on the Manhattan project. The name Monte Carlo was invented by John von Neumann and it references to the Monte Carlo Casino in Monaco (in a casino it is also the chance that arranges that after high number of repetitions it is the casino owner who wins the money; here the chance arranges that after high number of repetitions it is the physicist who wins the correct enough result).

There are a lot of different Monte Carlo methods but each of them has the same basic strategy. This strategy consists of three points:

- random generation of input from a predefined domain using a certain specified probability distribution
- performance of deterministic computation with the generated input
- aggregation and evaluation of the results obtained by individual computations

As every method based on chance, Monte Carlo technique gives results with required accuracy after high enough number of repetitions. Here we have to repeat the first two steps in order to get high enough statistics.

## 3.2 Monte Carlo in high energy physics

### 3.2.1 Basic structure of high-energy processes

Within the frame of quantum field theory all the process dynamics is described by Lorentz invariant matrix element. Nevertheless, the calculation of matrix element is so difficult that it has to be approximated by first few (often just one) terms of it's perturbative expansion. The main contribution comes from the first nontrivial term which is given by the so-called tree-level Feynman diagram. Contributions of higher-order terms are considered as (small) corrections. However, this perturbative treatment has it's limitations. One of them is the description of multiparton final state topologies because of the necessity of calculation of too many and too high-order terms within this approach. Some processes cannot be treated perturbatively at all because of large (running) coupling constant. In this case some additional approaches have to be used. Fortunately it turns out that the high-energy processes can be divided into several ("independent") parts. Thus the usually used structure scheme of high-energy process is the following:

- in case of colliding hadrons: determination of colliding partons momenta on the base of parton distribution functions
- initial-state radiation, i.e. branching of particles that appear in the hard process as initial-state particles (e.g. $q \to qg$, $e \to e\gamma, \ldots$)
- hard "skeleton" process given by (perturbatively calculated) matrix element
- final-state radiation, i.e. branching of particles that appear in the hard process as final-state particles
- hadronization, i.e. creation of real observable hadrons from final-state QCD partons

Nevertheless, the problem of high-energy process cannot be treated "on paper" (or at least it would be very difficult even in the simplest cases) although the simplifications are substantial. Therefore it is the role of Monte Carlo method to calculate predictions that would be comparable with experiment. The corresponding Monte Carlo based programs are called Monte Carlo event generators and could be imagined like (virtual) particle colliders (event producers).

Another large area where the Monte Carlo methods are widely used in high-energy physics is the detector simulation. Because the passage of particles through matter is statistical process it is very convenient to use statistics-based method to simulate it. Physicists use the detector simulations mainly to plan and optimize new detectors and their data analysis strategies. The event generators give the necessary input to detector simulations.

### 3.2.2 Pythia and Tauola

One of the most popular Monte Carlo event generators is Pythia. It offers a lot of hard processes simulations as well as initial and final-state radiation mechanism and a hadronization model (Lund string model). It also offers beam remnants treating (i.e. interactions of the partons that do not undergo hard process) which is of course necessary for the full collision simulation. In this thesis we used Pythia to generate Higgs boson in $pp$-collisions and it's decay into $\tau$-leptons. When treating $\tau$-lepton decays Pythia always assumes the $\tau$-leptons to be unpolarized and therefore to decay isotropically. For our purpose (study of angular distribution of $\tau$-leptons decay products) we had therefore to use some other program in addition. It's name is Tauola and it is inteded to treat $\tau$-leptons decays more precisely than Pythia. It therefore includes $\tau$ polarization effects. For more informations on Pythia see [9] or [10] which is valid even for great part of the Pythia 8 (C++ version) used while working on this thesis.

Tauola can be used with any MC generator that produces events with $\tau$-leptons and whose output is in HEPEVT or HepMC format. Tauola has two interfaces whose task is to prepare input parameters (with use of given event record) for Tauola program itself and to insert $\tau$-leptons decay products into the original event record. The two interfaces are the following:

- Tauola Fortran Interface: it's input is HEPEVT event record
- Tauola Universal C++ Interface: it's input is HepMC event record

. Tauola works in the following way:

- event record generated by some external MC generator is searched for $\tau$-leptons and $\tau$ neutrinos
- production vertex is identified for each particle found in the previous step; the particles are then grouped to pairs originating from the same vertex
- in case of $\tau$ production from the $Z/\gamma^*$ all the hard process leading to $\tau$ production should be reconstructed in order to calculate spin correlations correctly; sometimes this could be done only approximatively. In the case of $\tau$ production from the Higgs boson no information about the hard process is necessary thanks to the zero spin of this particle
- using all these informations the spin density matrix is (approximatively) calculated
- each $\tau$ pair is decayed with the spin effects included in the spin density matrix
- $\tau$-leptons decay products are written to the event record

More information on Tauola can be found in [11] or [12]. Information on how Tauola treats the polarization effects in $Z/\gamma^* \to \tau^-\tau^+$ production is in [13].

## 3.3 Simulation results

In this section we are going to present results obtained by simulation of $H/A \to \tau^-\tau^+ \to \pi^-/\rho^-\nu_\tau\pi^+/\rho^+\bar{\nu}_\tau$ decays. As stated above we used Pythia to generate Higgs boson production and it's decay to pair of $\tau$-leptons. And we used Tauola to perform the $\tau$-leptons decays. Because Higgs boson is spin-zero particle the angular distribution of it's decay products does not depend on the process leading to it's production. Thanks to this we could have chosen any process to produce the Higgs boson. We wanted, however, to simulate protons collisions so that it matched the real life case (LHC). As discussed in Section 1.1.2 there are four main Higgs boson QCD production processes in $pp$-collisions in MSSM. In our simulation we chose the process that is probably the most important for low values of $\tan\beta$ and that is of importance even in region of high values of this parameter, i.e. gluon-gluon fusion. We set the center-of-mass energy to 7 TeV. For the $Z$ boson production in 7 Tev center-of-mass $pp$-collisions we used the process of fermion-antifermion anihilation.

On Figures 3.1-3.6 there are histograms (distributions) of angle $\phi$ defined in Section 2.2. Figures 3.7 and 3.8 show 2-D distributions of variables $\cos\theta$ and $\cos\theta'$ for the case of Higgs boson (either CP-even or odd) and $Z$ boson decay. Nice comparison of the two distributions is in Figure 3.9. Figures 3.10 and 3.11 show 2-D distributions of pion energies in the decaying boson rest frame and in the laboratory frame for the case of Higgs boson and $Z$ boson decay respectively. Figure 3.12 shows the distributions of pions invariant masses for both cases of Higgs and $Z$ boson decays. The last Figure 3.13 shows comparison of two methods of signal and background differentiation (ROC curves for laboratory energies of pions and for pions invariant masses).

From Figures 3.1-3.6 we can see that the MC results match the (on the tree-level) predicted ones if we realize that the pictures show the angular distribution integrated over $\cos\theta$ and $\cos\theta'$, i.e. $(1/\Gamma)(\mathrm{d}\Gamma/\mathrm{d}\phi)$:

$$\frac{1}{\Gamma}\frac{\mathrm{d}\Gamma}{\mathrm{d}\phi} = \frac{1}{2\pi}\left(1 + S \times F \times \frac{\pi^2}{16}\cos\phi\right) \tag{3.1}$$

with $S$ and $F$ given by Table 2.1. Numerical values of the coefficient $S \times F \times \frac{\pi^2}{16}$ for individual cases are summarized in Table 3.1. The values obtained by MC simulation are presented in the Table 3.1 as well (they are obtained by the relation $p0/p1$ between the two fit parameters; the errors are estimated using standard techniques, see for example [14]).

| | CP-even Higgs boson | | CP-odd Higgs boson | |
|---|---|---|---|---|
| hadrons | theory | MC | theory | MC |
| $\pi^-\pi^+$ | -0.617 | -0.622 $\pm$ 0.005 | 0.617 | 0.615 $\pm$ 0.005 |
| $\rho^-\pi^+$ | -0.280 | -0.268 $\pm$ 0.005 | 0.280 | 0.274 $\pm$ 0.005 |
| $\rho^-\rho^+$ | -0.124 | -0.115 $\pm$ 0.005 | 0.124 | 0.129 $\pm$ 0.005 |

Table 3.1: Coefficients: theory and Monte Carlo

The difference between 2-D distributions of variables $\cos\theta$ and $\cos\theta'$ for Higgs boson and $Z$ boson is clearly visible from Figures (3.7 and 3.8). More discussion is in Section 2.5.

Distributons of energies in the decaying boson rest frames are very similar to those of $\cos\theta$, $\cos\theta'$ (3.7 and 3.8) because the pion energy in CMS of Higgs ($Z$) boson ($E$, $E'$ for $\pi^-$, $\pi^+$ respectively) is linear function of $\cos\theta$ in case of $\pi^-$ and of $\cos\theta'$ in case of $\pi^+$:

$$E = \gamma\left(p^0_{\mathrm{CMS}\tau^-} + \beta\,|\vec{p}_{\mathrm{CMS}\tau^-}|\cos\theta\right) \tag{3.2}$$

$$E' = \gamma\left(p'^0_{\mathrm{CMS}\tau^+} - \beta\left|\vec{p'}_{\mathrm{CMS}\tau^+}\right|\cos\theta'\right) \tag{3.3}$$

The distributions of pion energies in the laboratory rest frame differ for the case of Higgs and $Z$ boson as we can see from the Figures 3.10 and 3.11. In principle it is thus possible to distinguish the signal and background on the basis of experimentaly accessible pions energies in the laboratory frame.

The distributions of pions invariant masses (Figure 3.12) for both cases of Higgs and $Z$ boson decays differ too so that they could also be used to distinguish signal and background. From Figure 3.13 we can see that the signal and background differentiation is better to do on the basis of pions invariant masses than on the basis of their laboratory energies. The ROC curve for pions laboratory energies was made with respect to the cuts on sum of these energies. This curve is below the ROC curve for pions invariant masses on all the interval $(0, 1)$ which means that for any value of $Z$ events rejection we obtain higher Higgs efficiency with the invariant-mass-based method.

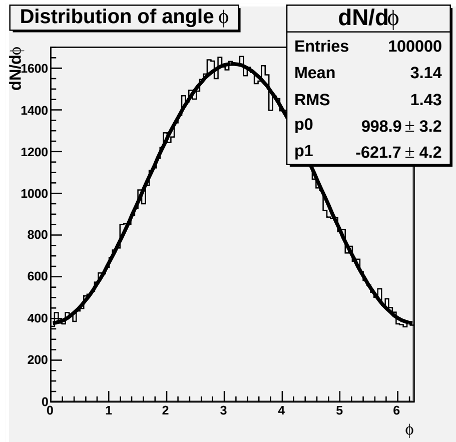


Figure 3.1: Distribution of angle $\phi$ in $H \to \tau^-\tau^+ \to \pi^-\nu_\tau\pi^+\bar{\nu}_\tau$ process.

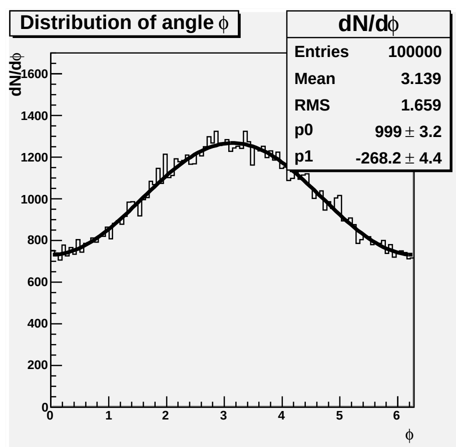


Figure 3.2: Distribution of angle $\phi$ in $H \to \tau^-\tau^+ \to \rho^-\nu_\tau\pi^+\bar{\nu}_\tau$ process.

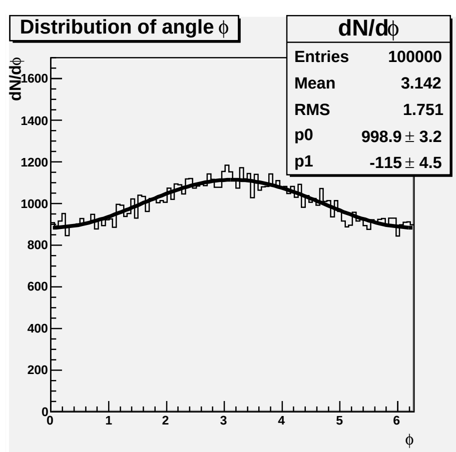


Figure 3.3: Distribution of angle $\phi$ in $H \to \tau^-\tau^+ \to \rho^-\nu_\tau\rho^+\bar{\nu}_\tau$ process.

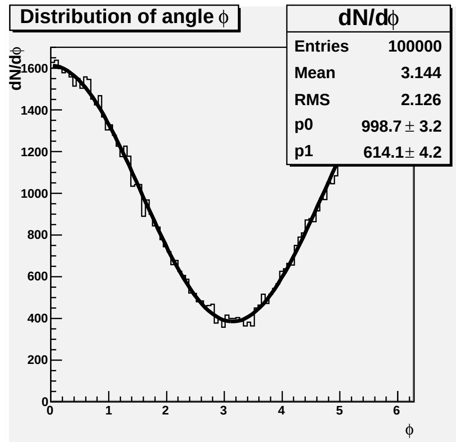


Figure 3.4: Distribution of angle $\phi$ in $A \to \tau^-\tau^+ \to \pi^-\nu_\tau\pi^+\bar{\nu}_\tau$ process.

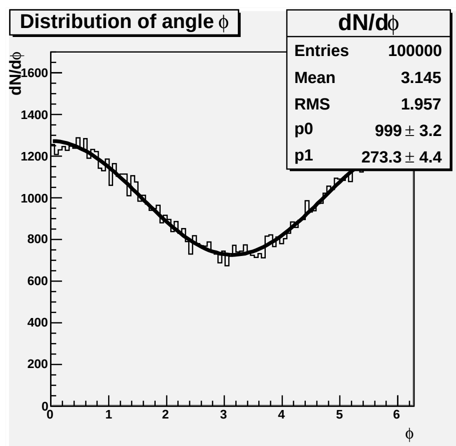


Figure 3.5: Distribution of angle $\phi$ in $A \to \tau^-\tau^+ \to \rho^-\nu_\tau\pi^+\bar{\nu}_\tau$ process.

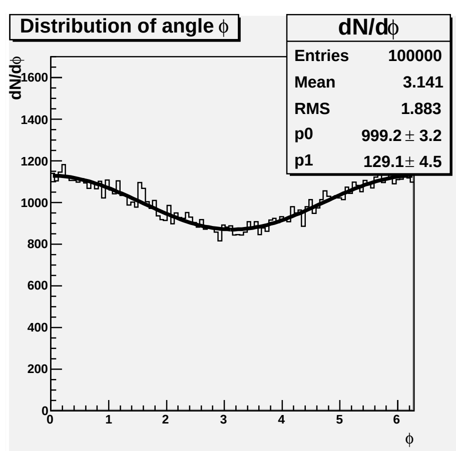


Figure 3.6: Distribution of angle $\phi$ in $A \to \tau^-\tau^+ \to \rho^-\nu_\tau\rho^+\bar{\nu}_\tau$ process.

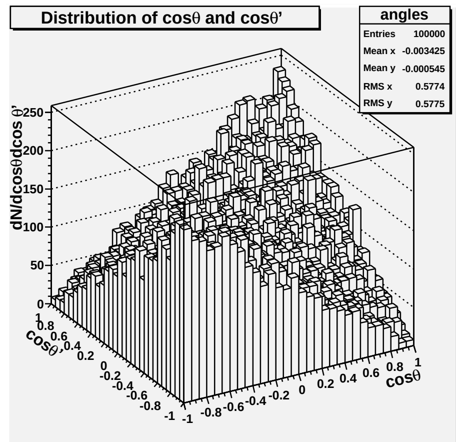


Figure 3.7: Distribution of variables $\cos\theta$ and $\cos\theta'$ in $H/A \to \tau^-\tau^+ \to \pi^-\nu_\tau\pi^+\bar{\nu}_\tau$ process.

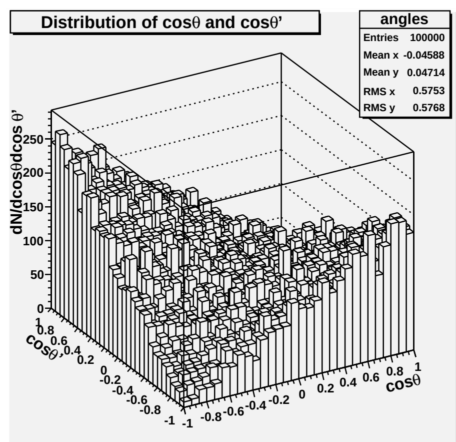


Figure 3.8: Distribution of variables $\cos\theta$ and $\cos\theta'$ in $Z \to \tau^-\tau^+ \to \pi^-\nu_\tau\pi^+\bar{\nu}_\tau$ process.

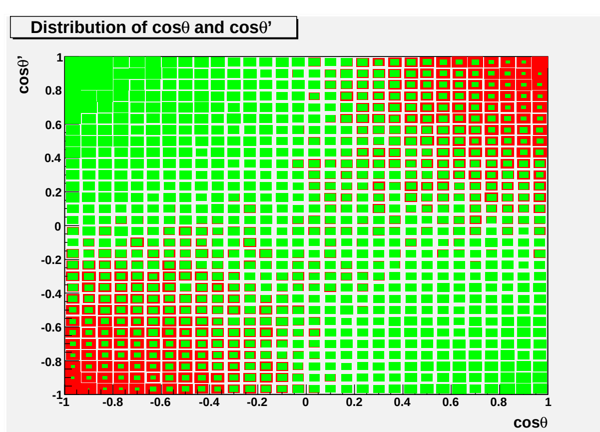


Figure 3.9: Distribution of variables $\cos\theta$ and $\cos\theta'$ for both $H/A \to \tau^-\tau^+ \to \pi^-\nu_\tau\pi^+\bar{\nu}_\tau$ (red) and $Z \to \tau^-\tau^+ \to \pi^-\nu_\tau\pi^+\bar{\nu}_\tau$ (green) processes.

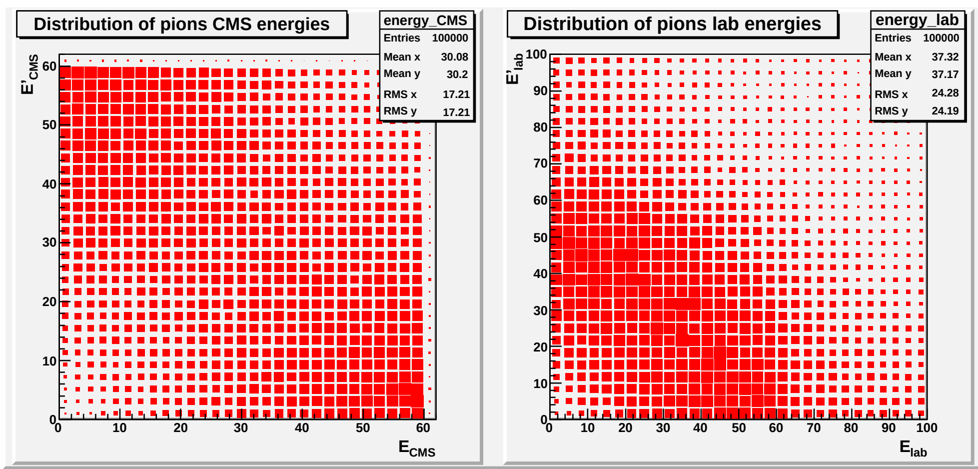


Figure 3.10: Distribution of pions energies $E$, $E'$ from $H/A \to \tau^-\tau^+ \to \pi^-\nu_\tau\pi^+\bar{\nu}_\tau$ process in CMS of Higgs boson and in laboratory frame.

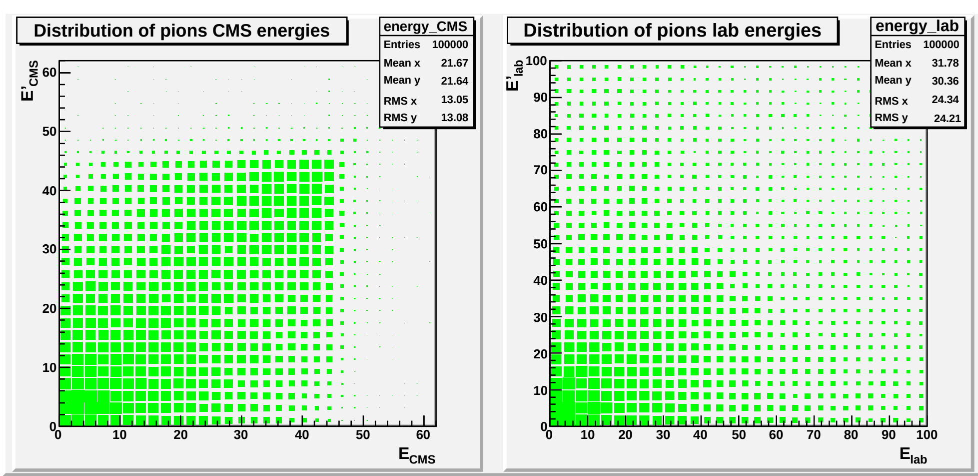


Figure 3.11: Distribution of pions energies $E$, $E'$ from $Z \to \tau^-\tau^+ \to \pi^-\nu_\tau\pi^+\bar{\nu}_\tau$ process in CMS of $Z$ boson and in laboratory frame.

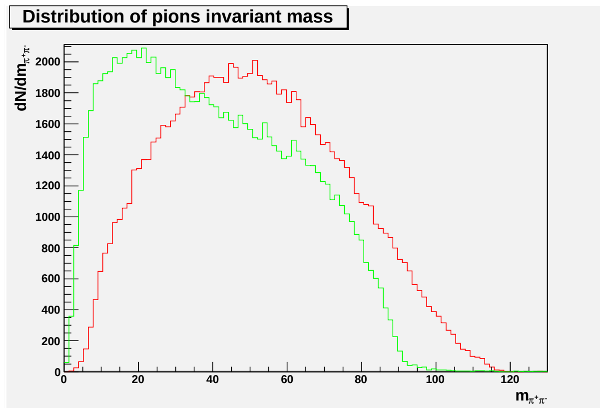


Figure 3.12: Distribution of pions invariant masses for the case of $H \rightarrow \tau^-\tau^+ \rightarrow \pi^-\nu_\tau\pi^+\bar{\nu}_\tau$ process (red) and $Z \rightarrow \tau^-\tau^+ \rightarrow \pi^-\nu_\tau\pi^+\bar{\nu}_\tau$ process (green).

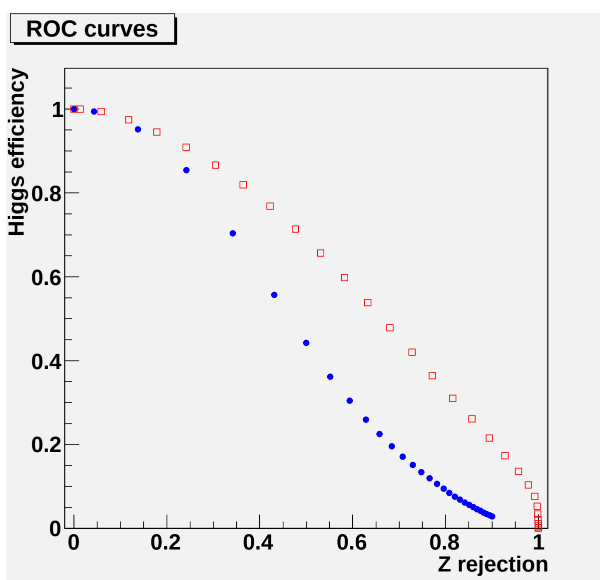


Figure 3.13: ROC curves for pions laboratory energies (blue) and pions invariant masses (red).

# Chapter 4

# Conclusions

In this diploma thesis the angular correlations of hadrons from decays $H/A \to \tau^-\tau^+ \to \pi^-/\rho^-\ \nu_\tau\ \pi^+/\rho^+\ \bar{\nu}_\tau$ were studied. Angular distributions of hadrons were calculated in the first non-trivial order of perturbation theory in the frame of MSSM. They were also calculated on the basis of general quantum-mechanical orbital momentum considerations. Results are summarized in equation (2.46) and in Table 2.1. The most important point is that the distributions for CP-even Higgs boson $H$ and for CP-odd one $A$ differ in the sign in front of the term that correlates transverse components of hadrons momenta.

We also studied the angular correlations in the decay $Z \to \tau^-\tau^+ \to \pi^-\nu_\tau\pi^+\bar{\nu}_\tau$ that represents the most important background in the region of not very high Higgs boson masses. We came to conclusion that in principle it is possible to distinguish this background process from the signal one with use of the correlation of longitudinal components of hadrons momenta - the sign in front of the term $\cos\theta\cos\theta'$. This different sign propagates to differences in the distributions of pions energies (Figures 3.10 and 3.11) and pions invariant masses (Figure 3.12).

Simulations of all the processes were made with use of MC generators Pythia 8 and Tauola. The simulation results are in agreement with our tree-level based theoretical results. It holds because Tauola uses the same angular distributions (see [15] with citation of [16]). However, we used different calculation techniques to recover these results.

# Appendix A

# Calculation based on angular momentum considerations

Here we are going to derive the angular distribution of pions from $h/A \to \tau^-\tau^+$, $\tau^\mp \to \pi^\mp\nu_\tau(\bar{\nu}_\tau)$ cascade decay on the basis of considerations about angular momentum. We are going to derive and numerically express the wave function of $\tau^-\tau^+$ pair born in decay of $H/A$. Then we will calculate the probability of finding neutrinos with general spin direction within such a wave function (the probability that a taoun decays into neutrino going in given direction is determined by scalar product of their spin functions). This will immediately give us the desired angular correlation of pions because neutrino's spin and momentum are correlated (neutrinos are left-handed and anti-neutrinos are right-handed) and the directions of momentum of pion and neutrino are opposite in $\tau$-lepton rest frames. Notation that we are going to use is the same as in all the thesis. In addition $\vec{n}$ will denote the orientation of spin of neutrino in $\tau^-$ rest frame, $\vec{n'}$ will denote the orientation of spin of anti-neutrino in $\tau^+$ rest frame. They can be expressed in terms of angles $\theta$, $\theta'$, $\phi$:

$$\begin{aligned} \vec{n} &= (\sin\theta, 0, \cos\theta) \\ \vec{n'} &= (-\sin\theta'\cos\phi, -\sin\theta'\sin\phi, -\cos\theta') \end{aligned} \tag{A.1}$$

First we find out which values of total spin are allowed for $\tau^-\tau^+$ pair. In the case of CP-even (CP-odd) Higgs boson, we know that the final state of it's decay products is CP-even (CP-odd) too. For a fermion-antifermion system we know that:

$$\mathrm{C}(f\bar{f}) = (-1)^{l+s} \tag{A.2}$$

$$\mathrm{P}(f\bar{f}) = (-1)^{l+1} \tag{A.3}$$

$$\mathrm{CP}(f\bar{f}) = (-1)^{s+1} \tag{A.4}$$

If we want the final state to be CP-odd, the total spin has to be 0 (CP conservation). It means that the relative orbital momentum has to be 0 as well (total angular momentum conservation; neutral Higgs boson have zero spin). If we want the final state to be CP-even, the total spin has to be 1. It means that the relative orbital momentum has to be 1 as well.

## A.1 CP-odd Higgs boson

Assuming that the $\tau$-lepton polarization is taken with respect to the $z$-axis we use the following notation ($|\tau^-_\uparrow\rangle$ denotes the spin function: the subscript says whether the spin aims in the direction of $z$-axis - $\uparrow$ - or in the opposite direction - $\downarrow$):

$$\begin{aligned} |\tau^-_\uparrow\rangle &= \begin{pmatrix} 1 \\ 0 \end{pmatrix}, \quad |\tau^-_\downarrow\rangle = \begin{pmatrix} 0 \\ 1 \end{pmatrix} \\ |\tau^+_\uparrow\rangle &= \begin{pmatrix} 1 \\ 0 \end{pmatrix}, \quad |\tau^+_\downarrow\rangle = \begin{pmatrix} 0 \\ 1 \end{pmatrix} \end{aligned} \tag{A.5}$$

The spin-angular part of the wave function of $\tau$-leptons born in the CP-odd Higgs boson decay is (as stated above total spin is 0 in this case and angular momentum is 0 too):

$$|\tau^+\tau^-\rangle \sim Y_0^0 \frac{1}{\sqrt{2}} \left( |\tau^-_\uparrow\rangle|\tau^+_\downarrow\rangle - |\tau^-_\downarrow\rangle|\tau^+_\uparrow\rangle \right) \tag{A.6}$$

Let us rotate the neutrino spin functions from frames where they are simple, i.e.

$$|\nu_{\mathrm{simp}}\rangle = \begin{pmatrix} 1 \\ 0 \end{pmatrix}, \quad |\bar{\nu}_{\mathrm{simp}}\rangle = \begin{pmatrix} 0 \\ 1 \end{pmatrix} \tag{A.7}$$

to respective $\tau$-lepton's rest frames (these simple neutrino spin functions are chosen such that the directions of $z$-axes of the rotated rest frames are the same as the pions momenta directions). Thus we obtain:

$$D^{(\frac{1}{2})}(0,\theta,0) = \begin{pmatrix} \cos\frac{\theta}{2} & -\sin\frac{\theta}{2} \\ \sin\frac{\theta}{2} & \cos\frac{\theta}{2} \end{pmatrix} \tag{A.8}$$

$$D^{(\frac{1}{2})}(\phi,\theta',0) = \begin{pmatrix} e^{-\frac{i}{2}\phi}\cos\frac{\theta'}{2} & -e^{-\frac{i}{2}\phi}\sin\frac{\theta'}{2} \\ e^{\frac{i}{2}\phi}\sin\frac{\theta'}{2} & e^{\frac{i}{2}\phi}\cos\frac{\theta'}{2} \end{pmatrix} \tag{A.9}$$

$$\begin{aligned} |\nu\rangle &= D^{(\frac{1}{2})}(0,\theta,0) \begin{pmatrix} 1 \\ 0 \end{pmatrix} = \begin{pmatrix} \cos\frac{\theta}{2} \\ \sin\frac{\theta}{2} \end{pmatrix} \\ |\bar{\nu}\rangle &= D^{(\frac{1}{2})}(\phi,\theta',0) \begin{pmatrix} 0 \\ 1 \end{pmatrix} = \begin{pmatrix} -e^{-\frac{i}{2}\phi}\sin\frac{\theta'}{2} \\ e^{\frac{i}{2}\phi}\cos\frac{\theta'}{2} \end{pmatrix} \end{aligned} \tag{A.10}$$

Now we have all we need to calculate the angular distribution:

$$\langle\nu|\langle\bar{\nu}| \left( |\tau^-\tau^+\rangle \right) \sim \langle\nu|\langle\bar{\nu}| Y_0^0 \frac{1}{\sqrt{2}} \left( |\tau^-_\uparrow\rangle|\tau^+_\downarrow\rangle - |\tau^-_\downarrow\rangle|\tau^+_\uparrow\rangle \right) \tag{A.11}$$

Using (A.7) and (A.10) we can write:

$$\langle\nu|\langle\bar{\nu}| \left( |\tau^-\tau^+\rangle \right) \sim Y_0^0 \frac{1}{\sqrt{2}} \left( \cos\frac{\theta}{2} e^{\frac{i}{2}\phi} \cos\frac{\theta'}{2} - \sin\frac{\theta}{2} \left( -e^{-\frac{i}{2}\phi} \sin\frac{\theta'}{2} \right) \right) \tag{A.12}$$

and consequently

$$\left|\langle\nu|\langle\bar{\nu}|\left(|\tau^-\tau^+\rangle\right)\right|^2 \sim \left|\mathrm{Y}_0^0\right|^2 \frac{1}{2}\Bigg(\cos^2\frac{\theta}{2}\cos^2\frac{\theta'}{2}+\sin^2\frac{\theta}{2}\sin^2\frac{\theta'}{2}+ \\ +2\mathrm{Re}\Bigg(\cos\frac{\theta}{2}\cos\frac{\theta'}{2}\sin\frac{\theta}{2}\sin\frac{\theta'}{2}e^{-i\phi}\Bigg)\Bigg) \tag{A.13}$$

After some simple manipulation with trigonometric functions and after institution $\mathrm{Y}_0^0 = 1/\sqrt{4\pi}$ we finally obtain:

$$\left|\langle\nu|\langle\bar{\nu}|\left(|\tau^-\tau^+\rangle\right)\right|^2 \sim \frac{1}{16\pi}(1+\cos\theta\cos\theta'+\sin\theta\sin\theta'\cos\phi) \tag{A.14}$$

And thus

$$\frac{1}{\Gamma}\frac{\mathrm{d}\Gamma}{\mathrm{d}\cos\theta\mathrm{d}\cos\theta'\mathrm{d}\phi} = \frac{1}{8\pi}(1+\cos\theta\cos\theta'+\sin\theta\sin\theta'\cos\phi) \tag{A.15}$$

## A.2 CP-even Higgs boson

The spin-angular part of wave function of $\tau$-leptons born in the CP-even Higgs boson decay is (as stated above total spin is 1 in this case and angular momentum is 1 too):

$$|\tau^-\tau^+\rangle \sim \frac{1}{\sqrt{3}}\left(\mathrm{Y}_1^1|\tau_\downarrow^-\rangle|\tau_\downarrow^+\rangle - \mathrm{Y}_1^0\frac{1}{\sqrt{2}}\left(|\tau_\uparrow^-\rangle|\tau_\downarrow^+\rangle + |\tau_\downarrow^-\rangle|\tau_\uparrow^+\rangle\right) + \mathrm{Y}_1^{-1}|\tau_\uparrow^-\rangle|\tau_\uparrow^+\rangle\right) \tag{A.16}$$

where $\mathrm{Y}_l^m = \mathrm{Y}_l^m(\theta^*,\phi^*)$ are functions of directions of $\tau$-leptons momenta in the Higgs boson rest frame. But we can choose the coordinate system arbitrarily. We choose it such that the $z$-axis of this system have the same direction as the momentum of negative $\tau$-lepton (which means that $\theta^* = 0$ and so $\mathrm{Y}_1^1 = \mathrm{Y}_1^{-1} = 0, \quad \mathrm{Y}_1^0 = \sqrt{\frac{3}{4\pi}}$). After this choice we can write:

$$|\tau^+\tau^-\rangle \sim -\frac{1}{\sqrt{8\pi}}\left(|\tau_\uparrow^-\rangle|\tau_\downarrow^+\rangle + |\tau_\downarrow^-\rangle|\tau_\uparrow^+\rangle\right) \tag{A.17}$$

After calculations analogic to those done in previous Section A.1 we finally obtain:

$$\left|\langle\nu|\langle\bar{\nu}|\left(|\tau^-\tau^+\rangle\right)\right|^2 \sim \frac{1}{16\pi}(1+\cos\theta\cos\theta'-\sin\theta\sin\theta'\cos\phi) \tag{A.18}$$

And thus

$$\frac{1}{\Gamma}\frac{\mathrm{d}\Gamma}{\mathrm{d}\cos\theta\mathrm{d}\cos\theta'\mathrm{d}\phi} = \frac{1}{8\pi}(1+\cos\theta\cos\theta'-\sin\theta\sin\theta'\cos\phi) \tag{A.19}$$

# Appendix B

# Detailed calculation of squared matrix element

## B.1 Squared matrix element

We are going to perform detailed calculation of the squared matrix element from Section 2.2.1. Process to be calculated is described by Feynman diagram 2.1. Corresponding matrix element is given by (2.9). It's complex conjugate is

$$\mathcal{M}^* \;=\; g_{H\tau\tau}(-G_F\cos\theta_C f_\pi)^2 \times 4\bar{v}_R(k')\not{p}'\frac{1}{-\not{q}'-m_\tau}\frac{1}{\not{q}-m_\tau}\not{p}u_L(k) \tag{B.1}$$

The squared matrix element is:

$$\begin{aligned}
|\mathcal{M}|^2 &= C\times\bar{v}_R(k')\not{p}'(-\not{q}'+m_\tau)(\not{q}+m_\tau)\not{p}u_L(k)\bar{u}_L(k)\not{p}(\not{q}+m_\tau)(-\not{q}'+m_\tau)\not{p}'v_R(k')\\
&= C\times\mathrm{Tr}\left(\not{k}'\frac{1+\gamma_5}{2}\not{p}'(-\not{q}'+m_\tau)(\not{q}+m_\tau)\not{p}\not{k}\frac{1+\gamma_5}{2}\not{p}(\not{q}+m_\tau)(-\not{q}'+m_\tau)\not{p}'\right)\\
&\qquad\left|\begin{array}{l}
(1-\gamma_5)(-\not{q}'+m_\tau)(\not{q}+m_\tau)=\\
\qquad=(1-\gamma_5)(-\not{q}'\not{q}+m_\tau^2)+(1-\gamma_5)m_\tau(-\not{q}'+\not{q})\\
\qquad=(-\not{q}'\not{q}+m_\tau^2)(1-\gamma_5)+m_\tau(-\not{q}'+\not{q})(1+\gamma_5)\\
(1-\gamma_5)(1+\gamma_5)=0\\
(1-\gamma_5)(1-\gamma_5)=2(1-\gamma_5)\\
(1+\gamma_5)(1+\gamma_5)=2(1+\gamma_5)
\end{array}\right|\\
&= C\times\mathrm{Tr}\left(\not{k}'\not{p}'m_\tau(-\not{q}'+\not{q})\not{p}\not{k}\frac{1+\gamma_5}{2}\not{p}\left((-\not{q}\not{q}'+m_\tau^2)+m_\tau(-\not{q}'+\not{q})\right)\not{p}'\right)\\
&= C\times\mathrm{Tr}\left(\not{k}'\not{p}'m_\tau(-\not{q}'+\not{q})\not{p}\not{k}\frac{1+\gamma_5}{2}\not{p}m_\tau(-\not{q}'+\not{q})\not{p}'\right)\\
&= C\times\mathrm{Tr}\left(\not{p}\not{k}\not{p}m_\tau(\not{q}-\not{q}')\not{p}'\not{k}'\not{p}'m_\tau(\not{q}-\not{q}')\frac{1+\gamma_5}{2}\right)
\end{aligned} \tag{B.2}$$

Using the energy-momentum conservation

$$\begin{aligned}
p &= q-k\\
p' &= q'-k'
\end{aligned} \tag{B.3}$$

and the fact that with good accuracy neutrino can be considered as being massless (i.e. $\not{k}\not{k} = k^2 = 0$) the last expression is equal to:

$$|\mathcal{M}|^2 = C \times m_\tau^2 \mathrm{Tr}\left(\not{q}\not{k}\not{q}(\not{q} - \not{q}')\not{q}'\not{k}'\not{q}'(\not{q} - \not{q}')\frac{1+\gamma_5}{2}\right) \tag{B.4}$$

In order to continue we recall the well known formulas from arithmetic of $\gamma$-matrices:

$$\begin{aligned}
\gamma_\mu\gamma_\nu &= -\gamma_\nu\gamma_\mu + 2g_{\mu\nu} && \text{(B.5a)}\\
\mathrm{Tr}(\gamma_\mu\gamma_\nu) &= 4g_{\mu\nu} && \text{(B.5b)}\\
\mathrm{Tr}(\gamma_\mu\gamma_\nu\gamma_5) &= 0 && \text{(B.5c)}\\
\mathrm{Tr}(\gamma_\mu\gamma_\nu\gamma_\rho\gamma_\sigma) &= 4(g_{\mu\nu}g_{\rho\sigma} - g_{\mu\rho}g_{\nu\sigma} + g_{\mu\sigma}g_{\nu\rho}) && \text{(B.5d)}\\
\mathrm{Tr}(\gamma_\mu\gamma_\nu\gamma_\rho\gamma_\sigma\gamma_5) &= 4i\epsilon_{\mu\nu\rho\sigma} && \text{(B.5e)}\\
\not{a}\not{a} &= a^2 && \text{(B.5f)}
\end{aligned}$$

Now we can finish the calculation and express the squared matrix element in terms of scalar products of particles momenta:

$$\begin{aligned}
|\mathcal{M}|^2 &= C \times m_\tau^2 \mathrm{Tr}\Big(\not{q}\not{k}\not{q}m_\tau^2\not{k}'m_\tau^2\frac{1+\gamma_5}{2} - \not{q}\not{k}m_\tau^2\not{q}'\not{k}'m_\tau^2\frac{1+\gamma_5}{2} -\\
&\quad -m_\tau^2\not{k}\not{q}m_\tau^2\not{k}'\not{q}'\frac{1-\gamma_5}{2} + m_\tau^2\not{k}m_\tau^2\not{q}'\not{k}'\not{q}'\frac{1-\gamma_5}{2}\Big)\\
&= C \times m_\tau^6 \mathrm{Tr}\Big(\frac{1}{2}\not{q}\not{k}\not{q}\not{k}' - \not{q}\not{k}\not{q}'\not{k}'\frac{1+\gamma_5}{2} -\\
&\quad -(-\not{q}\not{k} + 2(k\cdot q))(-\not{q}'\not{k}' + 2(k'\cdot q'))\frac{1-\gamma_5}{2} + \frac{1}{2}\not{k}\not{q}'\not{k}'\not{q}'\Big)\\
&= C \times m_\tau^6 \mathrm{Tr}\Big(\frac{1}{2}\not{q}\not{k}\not{q}\not{k}' + \frac{1}{2}\not{k}\not{q}'\not{k}'\not{q}' - \not{q}\not{k}\not{q}'\not{k}'\frac{1+\gamma_5}{2} - \not{q}\not{k}\not{q}'\not{k}'\frac{1-\gamma_5}{2} +\\
&\quad +2(k\cdot q)\not{q}'\not{k}'\frac{1-\gamma_5}{2} + \not{q}\not{k}2(k'\cdot q')\frac{1-\gamma_5}{2} - 2(k\cdot q)2(k'\cdot q')\frac{1-\gamma_5}{2}\Big)\\
&= C \times m_\tau^6\frac{1}{2}\mathrm{Tr}\Big(\not{q}\not{k}\not{q}\not{k}' + \not{k}\not{q}'\not{k}'\not{q}' - 2\not{q}\not{k}\not{q}'\not{k}' +\\
&\quad +2(k\cdot q)\not{q}'\not{k}' + 2(k'\cdot q')\not{q}\not{k} - 2(k\cdot q)2(k'\cdot q')\Big)\\
&= C \times m_\tau^6\frac{1}{2}4(2(q\cdot k)(q\cdot k') - m_\tau^2(k\cdot k') + 2(k\cdot q')(k'\cdot q') - m_\tau^2(k\cdot k') -\\
&\quad -2(q\cdot k)(q'\cdot k') + 2(q\cdot q')(k\cdot k') - 2(q\cdot k')(k\cdot q') +\\
&\quad +2(k\cdot q)(q'\cdot k') + 2(k'\cdot q')(q\cdot k) - 2(k\cdot q)2(k'\cdot q'))\\
&= C \times 2m_\tau^6(2(q\cdot k)(q\cdot k') + 2(k'\cdot q')(k\cdot q') + (2(q\cdot q') - 2m_\tau^2)(k\cdot k') -\\
&\quad -2(q\cdot k')(k\cdot q') - 2(q\cdot k)(q'\cdot k'))
\end{aligned} \tag{B.6}$$

## B.2 Scalar products

Now, we are going to evaluate scalar products (2.13) in terms of variables $\cos\theta$, $\cos\theta'$ and $\phi$. We are going to use the same notation as in Section 2.2.1.

Thanks to the energy-momentum conservation in the Higgs boson rest frame we have:

$$\begin{aligned} q_{\mathrm{CMS}H} &= \left(\tfrac{m_H}{2}, 0, 0, \sqrt{\tfrac{m_H^2}{4} - m_\tau^2}\right) \\ q'_{\mathrm{CMS}H} &= \left(\tfrac{m_H}{2}, 0, 0, -\sqrt{\tfrac{m_H^2}{4} - m_\tau^2}\right) \end{aligned} \tag{B.7}$$

The Lorentz transformations then give:

$$\begin{aligned} q^0_{\mathrm{CMS}\tau^+} &= \gamma\left(q^0_{\mathrm{CMS}H} - \beta' q^3_{\mathrm{CMS}H}\right) \\ q^3_{\mathrm{CMS}\tau^+} &= \gamma\left(q^3_{\mathrm{CMS}H} - \beta' q^0_{\mathrm{CMS}H}\right) \\ q'^0_{\mathrm{CMS}\tau^-} &= \gamma\left(q'^0_{\mathrm{CMS}H} - \beta q'^3_{\mathrm{CMS}H}\right) \\ q'^3_{\mathrm{CMS}\tau^-} &= \gamma\left(q'^3_{\mathrm{CMS}H} - \beta q'^0_{\mathrm{CMS}H}\right) \\ \beta &= \sqrt{1 - \tfrac{4m_\tau^2}{m_H^2}} \\ \gamma &= \tfrac{m_H}{2m_\tau} \end{aligned} \tag{B.8}$$

Therefore we can write:

$$\begin{aligned} (k \cdot q') &= k^0_{\mathrm{CMS}\tau^-} q'^0_{\mathrm{CMS}\tau^-} - \left|\vec{k}_{\mathrm{CMS}\tau^-}\right| q'^3_{\mathrm{CMS}\tau^-} \left(-\cos\theta\right) \\ &= \left|\vec{k}_{\mathrm{CMS}\tau^-}\right| \left(q'^0_{\mathrm{CMS}\tau^-} + q'^3_{\mathrm{CMS}\tau^-}\cos\theta\right) \\ &= \left|\vec{k}_{\mathrm{CMS}\tau^-}\right| \gamma \left(q'^0_{\mathrm{CMS}H} - \beta q'^3_{\mathrm{CMS}H} + \cos\theta\left(q'^3_{\mathrm{CMS}H} - \beta q'^0_{\mathrm{CMS}H}\right)\right) \\ &= \left|\vec{k}_{\mathrm{CMS}\tau^-}\right| \gamma \left(q'^0_{\mathrm{CMS}H}\left(1 - \beta\cos\theta\right) - q'^3_{\mathrm{CMS}H}\left(\beta - \cos\theta\right)\right) \\ &= \left|\vec{k}_{\mathrm{CMS}\tau^-}\right| \gamma \frac{m_H}{2}\left(1 - 2\beta\cos\theta + \beta^2\right) \end{aligned} \tag{B.9}$$

The calculation of $(k' \cdot q)$ in CMS of $\tau^+$ is analogic:

$$(k' \cdot q) = \left|\vec{k'}_{\mathrm{CMS}\tau^+}\right| \gamma \frac{m_H}{2}\left(1 + 2\beta\cos\theta' + \beta^2\right) \tag{B.10}$$

The evaluation of $(q \cdot q')$ is very simple:

$$(q \cdot q') = \frac{1}{2}\left(\left(q + q'\right)^2 - q^2 - q'^2\right) = \frac{m_H^2 - 2m_\tau^2}{2} \tag{B.11}$$

Now we will evaluate the last term: $(k \cdot k')$. To do that we are going to boost the vector $k'$ to the $\tau^-$ rest frame. This vector can be expressed in terms of $\theta'$ and $\phi$:

$$\begin{aligned} k'^0_{\mathrm{CMS}\tau^+} &= \left|\vec{k'}_{\mathrm{CMS}\tau^+}\right| \\ k'^1_{\mathrm{CMS}\tau^+} &= -p'^1_{\mathrm{CMS}\tau^+} = -\left|\vec{k'}_{\mathrm{CMS}\tau^+}\right| \sin\theta'\cos\phi \\ k'^2_{\mathrm{CMS}\tau^+} &= -p'^2_{\mathrm{CMS}\tau^+} = -\left|\vec{k'}_{\mathrm{CMS}\tau^+}\right| \sin\theta'\sin\phi \\ k'^3_{\mathrm{CMS}\tau^+} &= -p'^3_{\mathrm{CMS}\tau^+} = -\left|\vec{k'}_{\mathrm{CMS}\tau^+}\right| \cos\theta' \end{aligned} \tag{B.12}$$

The vector $k_{\mathrm{CMS}\tau^-}$ is given by:

$$\begin{array}{rclcl} k^0_{\mathrm{CMS}\tau^-} & = & \left|\vec{k}_{\mathrm{CMS}\tau^-}\right| & & \\ k^1_{\mathrm{CMS}\tau^-} & = & -p^1_{\mathrm{CMS}\tau^-} & = & -|\vec{k}_{\mathrm{CMS}\tau^-}|\sin\theta \\ k^2_{\mathrm{CMS}\tau^-} & = & -p^2_{\mathrm{CMS}\tau^-} & = & 0 \\ k^3_{\mathrm{CMS}\tau^-} & = & -p^3_{\mathrm{CMS}\tau^-} & = & -|\vec{k}_{\mathrm{CMS}\tau^-}|\cos\theta \end{array} \tag{B.13}$$

We have to calculate the relative speed of tauons - in other words the speed $\beta^{\mathrm{CMS}\tau^+}_{\tau^-}$ of $\tau^-$ in $\tau^+$ rest frame:

$$\beta^{\mathrm{CMS}\tau^+}_{\tau^-} = \frac{\beta - \beta'}{1 - \beta\beta'} = \frac{2\beta}{1+\beta^2} \tag{B.14}$$

And the corresponding $\gamma$-factor:

$$\gamma^{\mathrm{CMS}\tau^+}_{\tau^-} = \frac{1+\beta^2}{1-\beta^2} \tag{B.15}$$

We can finally express $(k \cdot k')$ in terms of variables $\cos\theta$, $\cos\theta'$ and $\phi$:

$$\begin{aligned} (k \cdot k') \quad = \quad & \left|\vec{k}_{\mathrm{CMS}\tau^-}\right|\left|\vec{k'}_{\mathrm{CMS}\tau^+}\right| \times \left(\frac{1+\beta^2}{1-\beta^2}(1 - \cos\theta\cos\theta') + \right. \\ & \left. + \frac{2\beta}{1-\beta^2}\left(\cos\theta' - \cos\theta\right) - \sin\theta\sin\theta'\cos\phi\right) \end{aligned} \tag{B.16}$$

In case of $\pi^-$ in final state we have

$$|\vec{p}_{\mathrm{CMS}\tau^-}| = \left|\vec{k}_{\mathrm{CMS}\tau^-}\right| = k^0_{\mathrm{CMS}\tau^-} \quad = \quad \frac{m_\tau^2 - m_\pi^2}{2m_\tau} \tag{B.17a}$$

$$p^0_{\mathrm{CMS}\tau^-} \quad = \quad \frac{m_\tau^2 + m_\pi^2}{2m_\tau} \tag{B.17b}$$

and in case of $\rho^-$ in final state the pion mass is replaced by $\rho$-meson mass. Analogic expressions are of course valid for $\pi^+$ and $\rho^+$.

## B.3 Integration of the squared matrix element

We use standard techniques of integration over the Lorentz invariant phase space of four particles $\mathrm{LIPS}_4$:

$$\mathrm{dLIPS}_4 \quad = \quad (2\pi)^4\delta^4(h - p - k - p' - k')\frac{\mathrm{d}^3p}{(2\pi)^3 2p_0}\frac{\mathrm{d}^3k}{(2\pi)^3 2k_0}\frac{\mathrm{d}^3p'}{(2\pi)^3 2p'_0}\frac{\mathrm{d}^3k'}{(2\pi)^3 2k'_0} \tag{B.18}$$

$$\mathrm{d}\Gamma \quad = \quad \frac{1}{2m_H}|\mathcal{M}|^2\mathrm{dLIPS}_4 \tag{B.19}$$

where $h$ denotes the Higgs boson momentum. Well known relation between $\mathrm{dLIPS}_4$ and $\mathrm{dLIPS}_2$ is:

$$\begin{aligned} \mathrm{dLIPS}_4(M \to m_1 + m_2 + m_3 + m_4) = \frac{1}{(2\pi)^2}\mathrm{dLIPS}_2(M \to m_{12} + m_{34}) \times \\ \times\, \mathrm{dLIPS}_2(m_{12} \to m_1 + m_2)\ \mathrm{dLIPS}_2(m_{34} \to m_3 + m_4)\mathrm{d}m_{12}^2\mathrm{d}m_{34}^2 \end{aligned} \tag{B.20}$$

$\mathrm{dLIPS}_2$ is given by:

$$\mathrm{dLIPS}_2(m_{12} \to m_1 + m_2) \;=\; \frac{1}{16\pi^2}\frac{|\vec{p}_{\mathrm{CMS}}|}{m_{12}}\mathrm{d}\cos\theta\mathrm{d}\phi \tag{B.21}$$

where $|\vec{p}_{\mathrm{CMS}}|$ is magnitude of center-of-mass momentum and $\theta$, $\phi$ are center-of-mass spherical coordinates. Thanks to these relations we can write:

$$\begin{aligned} \mathrm{d}\Gamma &= \frac{1}{2m_H}|\mathcal{M}|^2\frac{1}{(2\pi)^2}\mathrm{dLIPS}_2(m_H \to m_{12} + m_{34}) \times \\ &\quad \times\mathrm{dLIPS}_2(m_{12} \to m_{\pi^-} + m_\nu)\ \mathrm{dLIPS}_2(m_{34} \to m_{\pi^+} + m_{\bar{\nu}})\mathrm{d}m_{12}^2\mathrm{d}m_{34}^2 \\ &= f(\theta, \theta', \phi)\delta(m_{12}^2 - m_\tau^2)\delta(m_{34}^2 - m_\tau^2)\ \mathrm{dLIPS}_2(m_H \to m_{12} + m_{34}) \times \\ &\quad \times\mathrm{dLIPS}_2(m_{12} \to m_{\pi^-} + m_\nu)\ \mathrm{dLIPS}_2(m_{34} \to m_{\pi^+} + m_{\bar{\nu}})\mathrm{d}m_{12}^2\mathrm{d}m_{34}^2 \\ &= f(\theta, \theta', \phi)\frac{4}{(8\pi)^4}\sqrt{1 - \frac{4m_\tau^2}{m_H^2}}\ \frac{|\vec{p}_{\mathrm{CMS}\tau^-}|}{m_\tau}\frac{\left|\vec{p'}_{\mathrm{CMS}\tau^+}\right|}{m_\tau}\mathrm{d}\cos\theta\mathrm{d}\cos\theta'\mathrm{d}\phi \end{aligned} \tag{B.22}$$

# Bibliography


[1] ATLAS Collaboration: *Expected Performance of the ATLAS Experiment, Detector, Trigger and Physics* (CERN-OPEN-2008-020, December 2008)

[2] J .Hořejší: *Fundamentals of Electroweak Theory* (The Karolinum Press, Prague 2002)

[3] ALEPH, DELPHI, L3, OPAL Collaborations, The LEP Working Group for Higgs Boson Searches: *Search for The Standard Model Higgs Boson at LEP* (Physics Letters B 565 (2003) 6175)

[4] The ALEPH, CDF, D0, DELPHI, L3, OPAL, SLD Collaborations, the LEP Electroweak Working Group, the Tevatron Electroweak Working Group and the SLD electroweak and heavy flavor groups: *Electroweak Measurements and Constraints on the Standard Model* (CERN-PH-EP-2010-095), http://lepewwg.web.cern.ch/LEPEWWG/stanmod/summer2010/s10_ew.pdf

[5] Particle Data Group Collaboration, K. Nakamura et al. (Journal of Physics G37 (2010) 075021)

[6] M. Dress, R. Godbole, P. Roy: *Theory and Phenomenology of Sparticles* (World Scientific Publishing Co. Pte. Ltd., 2004)

[7] I. Aitchison: *Supersymmetry in Particle Physics* (Cambridge University Press, Cambridge 2007)

[8] Georgios Dedes: *Study of the Higgs Boson Discovery Potential in the Process* $pp \to H/A \to \mu^+\mu^-/\tau^+\tau^-$ *with the ATLAS Detector* (dissertation, Technische Universitat Munchen, 2008, available at http://mediatum2.ub.tum.de/node?id=645838)

[9] http://home.thep.lu.se/∼torbjorn/Pythia.html

[10] T. Sjöstrand, S. Mrenna, P. Skands: *Pythia 6.4 Physics and Manual* (http://home.thep.lu.se/*sim*torbjorn/pythia/lutp0613man2.pdf)

[11] N. Davidson, G. Nanava, T. Przedzinski, E. Richter-Was, Z. Was: *Universal Interface of TAUOLA* (IFJPAN-IV-2009-10, January 2010)

[12] P. Golonka, B. Kersevan, T. Pierzchala, E. Richter-Was, Z. Was, M. Worek: *The tauola-photos-F environment for the TAUOLA and PHOTOS packages, release II* (CERN-TH/2003-287, December 2003)

[13] T. Pierzchala, E. Richter-Was, Z. Was, M. Worek: *Spin effects in tau-lepton pair production at LHC* (TPJU 2/2001)

[14] B. Sprušil, P. Zielencová: *Úvod do teorie fyzikálních měření* (SPN, Prague 1989)

[15] Z. Was, M. Worek: *Transverse spin effects in* $H/A \to \tau^-\tau^+; \tau^\pm \to \nu X^\pm$*, Monte Carlo approach* (Acta Physica Polonica B 33/7(2002), 1875-1884)

[16] M. Krämer, J. Kühn, M. L. Stong, P. M. Zerwas: *Prospects of measuring the parity of Higgs particles* (DESY 93-174, TTP 93-41, December 1993)